

AMERICAN UNIVERSITY OF BEIRUT

Dynamic Origins of Entropic Force:
Thermodynamic Theory vs. Molecular Dynamics
Simulations

by

LAMA HANNA TANNOURY

A thesis

submitted in partial fulfillment of the requirements
for the degree of Master of Science
to the Department of Physics
of the Faculty of Arts and Sciences
at the American University of Beirut

Beirut, Lebanon
January 2017

AMERICAN UNIVERSITY OF BEIRUT

Dynamic Origins of Entropic Force: Thermodynamic Theory vs. Molecular Dynamics Simulations

by
Lama Hanna Tannoury

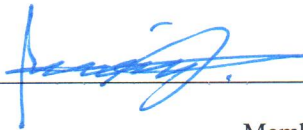
Approved by:



Dr. Leonid Klushin, Professor

Advisor

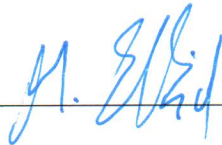
Physics



Dr. Jihad Touma, Professor

Member of Committee

Physics



Dr. Mounib El Eid, Professor

Member of Committee

Physics



Date of thesis defense: January 27, 2017

AMERICAN UNIVERSITY OF BEIRUT

THESIS, DISSERTATION, PROJECT RELEASE FORM

Student Name: Tannoury Lama Hanna
Last First Middle

Master's Thesis Master's Project Doctoral Dissertation

I authorize the American University of Beirut to: (a) reproduce hard or electronic copies of my thesis, dissertation, or project; (b) include such copies in the archives and digital repositories of the University; and (c) make freely available such copies to third parties for research or educational purposes.

I authorize the American University of Beirut, to: (a) reproduce hard or electronic copies of it; (b) include such copies in the archives and digital repositories of the University; and (c) make freely available such copies to third parties for research or educational purposes after : **One --- year from the date of submission of my thesis, dissertation, or project.**
Two --- years from the date of submission of my thesis, dissertation, or project.
Three --- years from the date of submission of my thesis, dissertation, or project.



Signature

30-1-2017

Date

This form is signed when submitting the thesis, dissertation, or project to the University Libraries

Acknowledgements

“Would you tell me, please, which way I ought to go from here?” - Alice

“That depends a good deal on where you want to get to,” said the cat

— Lewis Carroll, Alice’s Adventures in Wonderland

Just like Alice, I started my journey not knowing exactly where to go and which steps to tread. I stepped in for an adventure taking me to wonderland and I never imagined it would be a rollercoaster ride. It leaves you scared yet excited. Your heart races at every steep incline and at each drop you promise you would never do this again, yet at the end all you want to do is buy another ticket and go for a second ride. Yet my ride would never have been this fun and bearable without a group of people. Joumana, I would like to thank you for every deadline and course you’ve reminded me of and for everytime you had a solution for our problems. A great thank you goes to my friends especially to Rodrique and Antranik. Thank you for every intellectual, scientific and non-sensical conversation we’ve ever had. You have contributed greatly to the evolution of my thoughts. Thank you for always listening to my theories even when you did not have the time to.

To my advisor, Professor Klushin, I am forever grateful. You are the definition of a teacher. You have not only educated me in the physical sciences, your way of thinking has taught me how to analyze, study and dissect all the problems I could face. From the day I took my first undergraduate course with you 4 years ago till today, thank you for everything.

To my sisters, Hiba and Sana, whom I always look up to, thank you for being such great role models.

To Sana and Jeff, thank you for the full time moral support and for the jokes to cheer me up. Thank you for the endless conversations, for being part of my family and my close friends.

Finally, to mom and dad, not enough words can express my gratitude. Without you I would never be the person I am today.

I dedicate all of this to you.

An Abstract of the Thesis of

Lama Hanna Tannoury for Master of Science
Major: Physics

Title: Dynamic Origins of Entropic Force:

Thermodynamic Theory vs. Molecular Dynamics Simulations

The aim of this research is to study the dynamic origins of entropic forces acting on semi-confined polymer chains. We make use of Molecular Dynamics Simulations to study at first the global chain characteristics and relaxation times of fully confined chains. Our results infer that we need to go to higher values of N and stronger confinement to reach the asymptotic limits of the relaxation times and the radial forces acting on the chain. We eventually move on to study the dynamics of semi-confined chains in two limiting cases. The results show that for both cases (infinite and finite walls at the open end of the nanopore), the pulling force is only dependent on the temperature T and the diameter D with $f_{pull} \sim \tilde{B}k_B T/D$. Our model proves to be in agreement with the theoretical predictions which state that the two limiting cases should produce the same entropic force for given values of T and D . The value of \tilde{B} is extracted it appears that for semi-confined chains the pulling force's coefficient is different than the universal model independent constant $B = 5.79$. Studies of the effect of the length of the tail outside the nanopore were also administered. The change of weights/concentrations of contacts and magnitudes of forces with the radial distance were deduced from the Green's function of a polymer near a plane and were found to match our simulation results, and a final expression was obtained from the weights that retrieves the force's dependence on D theoretically. Finally, we provide a brief comparison of our model to the ejection of a dsDNA from a bacteriophage T5.

Contents

Acknowledgements	v
Abstract	vi
1 Introduction	1
2 Theoretical Background	5
2.1 The Free Polymer Chain	5
2.1.1 The Ideal Chain - A drunkard's walk	6
2.1.2 The Real Chain	9
2.1.3 Relaxation Times - A Harmonic Oscillator Approach	11
2.2 The Locked Up Polymer Chain	13
2.3 A Semi-Confined Polymer	16
3 Molecular Dynamics Simulations	18
3.1 Equations of Motion	18
3.2 Verlet Methods	20
3.2.1 Velocity Verlet	21
3.2.2 Numerical Scheme	22
3.3 Forces	23
3.3.1 Non-Bonded Interactions	23
3.3.2 Bonded Interactions	24
4 Our Own Adventure - The Road Taken	25
4.1 Infinitely Long Pore	26
4.2 Assembling our Limiting Cases	27
4.2.1 Infinite Outer Boundaries	27
4.2.2 Finite Outer Boundaries	28
4.2.3 The Inner and Outer Edges	29
4.3 Fixing the Polymer	30
4.4 Correlation Functions and Relaxation Times	32

5	Results and Analysis	34
5.1	Free Polymer Chain	34
5.2	The Fully Confined Polymer Chain	36
5.2.1	Average chain size characteristics	36
5.2.2	Relaxation time measurements	38
5.2.3	Free energy and force	39
5.3	The Semi-Confined Polymer Chain	43
5.3.1	Pulling Force	44
5.3.2	Radial Force	51
5.3.3	Confined Pull	52
5.3.4	Relation between radial and pulling force	54
5.3.5	Effects of the tail	55
6	Polymer Near a Plane	58
6.1	"Grafted" Chain to a Non-Adsorbing Wall	58
6.1.1	The Loop	60
6.1.2	The Tail	61
6.1.3	Weight of Contact	62
6.2	Comparison with MD results	63
7	A Brief Analogy to Biological Systems	70
8	Summary, Conclusion and Future Work	73
	References	77

List of Figures

2.1	The atomic structure of a polyethylene structure (left). The polymer chain as a long flexible string (right) [1].	6
2.2	Random walk of a polymer chain on a two dimensional lattice [2] . . .	7
3.1	Diagram for an MD simulation algorithm [3]	19
4.1	Sketch for a semi-confined polymer chain with infinite outer boundaries (large difference between D_{in} and D_{out})	28
4.2	Sketch for a semi-confined polymer chain with finite outer boundaries (small difference between D_{in} and D_{out})	29
4.3	Histogram showing the frequency of the magnitudes of the force exerted by the spring on the fixed monomer	31
5.1	Plot of the end-to-end distances R_{ee} and R_{ee}^2 for a free polymer chain for different number of monomers N.	35
5.2	Plot of the relaxation times τ_{rel} for a free polymer chain for different number of monomers N.	36
5.3	Power law governing R_{ee} (a) and R_{ee}^2 (b) dependence on N.	37
5.4	Power law governing R_{ee} (a) and R_{ee}^2 (b) dependence on D.	37
5.5	(a) shows the dependence of the relaxation times on N. (b) shows the dependence of the relaxation times on the effective diameter.	38
5.6	Variation of f_{radial} with the scaling variable $(2/\nu)ND_{eff}^{-2.6}$	40
5.7	Variation of f_{radial} with the scaling variable $(2/\nu)N^{0.78}D_{eff}^{-2.3}$	41
5.8	Variation of f_{radial}/R_{ee} with $(2/\nu)N^{-0.22}D^{-1.7}$ produces the constant B.	42
5.9	Finite Boundary: The dependence of f_{pull} on D_{eff} for $N = 150, 200, 300$ in (a) , (b), and (c) respectively.	46
5.10	Infinite Boundary: The dependence of f_{pull} on D_{eff} for $N = 150, 200, 300$ in (a) , (b), and (c) respectively.	47
5.11	The dependence of the pulling force on the temperature T for $T = 1/2, 1, 2, 5, 7$	48
5.12	For infinite boundaries and for different values of N, we plot f_{pull} against $1/D_{eff}$ to extract the coefficient B	49

5.13	For finite boundaries and for different values of N , we plot f_{pull} against $1/D_{eff}$ to extract the coefficient B	50
5.14	Plot of f_{radial} against $\frac{2L}{D^2}$ for a semi-confined chain produces the coefficient B	51
5.15	Plot of f_{radial} against f_{pull} for a semi-confined chain.	55
5.16	Pulling force as a function of the size of the tail.	57
6.1	Sketch of a grafted polymer chain near a non-adsorbing surface	60
6.2	The Concentration of forces (a) and contacts (b) of interaction for $N = 300$ and $D = 5$ for infinite and finite outer boundaries	65
6.3	The Concentration of forces (a) and contacts (b) of interaction for $N = 300$ and $D = 7$ for infinite and finite outer boundaries	66
6.4	The Concentration of forces (a) and contacts (b) of interaction for $N = 300$ and $D = 12$ for infinite and finite outer boundaries	67
6.5	$Log_{10} - Log_{10}$ plot of the force concentration against the radial distance for $N = 200 / D = 10$ with finite boundaries of different thicknesses	68
6.6	A plot of the densities of monomers near the open end of the tube along the radial direction for $D = 5,7,10,12$	69
7.1	A 2D and 3D image of the structure of a bacteriophage	71

List of Tables

5.1	Pulling Force (Infinite Boundaries)	44
5.2	Pulling Force (Finite Boundaries)	44
5.3	Pulling Force dependence on T	46
5.4	Data for Confined Pull	53
5.5	Data for radial force and pulling force for N=300 for semi-confined chain	54
5.6	The length of the polymer inside the tube in terms of the total number of blobs	57

Chapter 1

Introduction

Polymers in solutions and in confined spaces have acquired a large amount of interest in many areas of science. The pioneer in the field of polymer physics is P.J. Flory, whose work laid down the building blocks for scientists to come. One of the countless contributions of Flory's studies was the universal law concerning the exponent ν that changes with dimensionality d , upon which numerous power laws defining the chains characteristics are based. Furthermore, the Flory theory of polymers in good solvents introduced the idea of an excluded volume parameter ν for real chains which in turn played a role in the birth of the expression of the free energy of real polymer chains [4]. From the latter, he was able to deduce the power law governing the dependence of the chain size of a free polymer to the degree of polymerization N (refer to §2.1.2).

Other great pioneers in the field of polymer physics and their scaling concepts are P.G. de Gennes and M. Daoud. In a paper regarding the statistics of macromolecular solutions trapped in small pores [5], they study the scaling theory behind a chain trapped in a slit and in a capillary, as well as the features of multiple chains and their overlapping in confinement. They bring forth the concept of blobs and blob theory (re-

fer to §2.2) to set up the scaling arguments of the free energy and the length of trapped real chains, where T is the temperature, D is the diameter of confinement (cylindrical in our case) and B is a model-independent constant of value 5.79.

$$F_{conf} = \frac{Bk_B T}{D} R_{conf} \quad (1.1)$$

The above equation is the core of our research. Previous studies on the dynamics of a polymer confined within a nanopore have shown that a fully confined flexible chain experiences only random thermal kicks with zero mean resulting in a diffusive center-of-mass motion; in contrast to that, a partially confined long polymer with a tail outside the pore is subject to a steady mean ejecting force; derived from the free energy equation. It is well known that confining a flexible polymer chain inside a narrow tube leads to a reduction in configurational entropy and a corresponding increase in the free energy [6]. Translation along an infinitely long tube does not result in a change in free energy and thus does not generate a mean force. However, the free energy of a partially confined chain is reduced if the inner chain end is displaced towards the tube opening and more monomers escape the confinement. This free energy is that stated above and can be rewritten as:

$$F = \frac{Bk_B T}{D} x \quad (1.2)$$

where x is the distance from the inner chain end to the tube opening, or in other words the length of the confined part of the chain, D is the tube diameter, k_B is the Boltzmann constant, T is the temperature, and B is a numerical prefactor close ~ 5 as predicted by Monte-Carlo simulations and renormalization-group theory [7]. This implies that the inner end of the chain that is fixed in space should experience a mean reaction force of the following magnitude:

$$f = \frac{Bk_B T}{D} \quad (1.3)$$

In this equation, we can see that the force depends on the temperature and the diameter of the pore. Consequently, the force is predicted to be independent of the total length of the pore, the length of the tail of the chain outside the pore and the details of the boundaries at the open end of the tube.

Our aim, in this thesis, is to make use of molecular dynamics simulations to study the dynamic origins of the entropic force and the effects due to the boundary shape and the length of the tail. We take our nanopore to be a cylindrical tube of length L with one end closed and the other one open. The chain end at the closed part is fixed at a distance $x = L$ from the open end. The tube has an inner diameter D_{in} and an outer diameter D_{out} . Then, we consider two limiting cases arising from the difference between these two diameters. The first limiting case has a very large difference between both diameters, and accordingly we can think of the flat edge surface at the open end of the tube as one that extends infinitely. On the other hand, in the second case, we take the difference between the diameters to be very small. Due to that, the polymer tail is free to access the space beyond the outer cylinder surface of the tube.

In a dynamical setting, the net instantaneous force that acts on all monomers can have an axial (horizontal in our case) component only as a result to the monomers' collisions with the flat edge surface. The collisions with the inner and outer side walls can only produce radial forces. Thus if one is to examine the two limiting cases, it would seem natural that the frequency of collisions in the case of the infinite boundary should exceed that of the finite boundary. From this perspective, one would deduce that there would be a measurable difference in the magnitude of the mean ejection force. How-

ever, theoretical predictions based on equilibrium entropy considerations suggests that the mean ejection forces that emerge in the two limiting cases are the same and should be given by eq.(1.3).

Now, we direct our study at certain goals. First, we intend to check how numerical simulations agree with the theory [7, 8, 9] concerning global equilibrium statistics and average chain size characteristics in fully confined chains. Concerning dynamic scaling and relaxation times specifically, the theoretical scaling [10] has not been directly confirmed by simulations, and MC and MD simulations administered by Arnold et al. [11], have given different scaling laws than those of the theory. However, we will proceed to study our model's dynamic scaling and compare to those of the theory and other simulations. Subsequently, we proceed to explore the semi-confined chain and the resultant entropic force from the two limiting cases along with the change of the latter with different sizes of the tail.

Before we present our results, a theoretical background of the subject is provided.

Chapter 2

Theoretical Background

2.1 The Free Polymer Chain

A polymer which is etymologically written as (poly)-(mer) is translated from Greek as (many)-(parts) and refers to macromolecules consisting of several repeating units. These units are called monomers and are covalently (chemically) bonded to each other in a process called *polymerization* during which the structure of a polymer is attained. One of the basic characteristics of a polymer is the number of monomers in the chain and is known as the *degree of polymerization* N . Depending on the nature of the polymer's repeating units, we can define two types of chains. *Homopolymers* are molecules consisting of monomers which are made of identical repeating units. The second type of macromolecules is *heteropolymers*. The latter is a combination of different types of monomers into one chain. Biopolymers such as **DNA** are heteropolymers. They are fabricated from four different types of monomers known as *nucleotides*. As for proteins, also an example of biopolymers, they can be broken down to 20 distinct types of monomers (amino acids) [12].

Different types of interactions arise from various constraints administered on the

polymer chain. However, if we consider a free homopolymer chain with only covalent-bond interactions, we end up with the simplest form known as ideal chains.

2.1.1 The Ideal Chain - A drunkard's walk

The drunkard's walk, or most commonly known as the simple random walk is one of the models used to obtain a general picture of an ideal chain's characteristics. We make the following assumption: our chain has a high degree of flexibility and is allowed to take on several configurations. As a consequence of that, we are able to depict our polymer as a long string as in fig.(2.1).

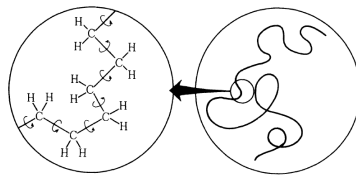


Figure 2.1: The atomic structure of a polyethylene structure (left). The polymer chain as a long flexible string (right) [1].

According to the drunkard's walk, our polymer chain follow a regular lattice seen in fig (2.2).In this picture, all directions taken by the chain have the same probability and our chain's movement along the lattice conforms with that of a random walk, thus making it possible for us to exploit the latter's statistical properties to derive those related to our chain.

Let \mathbf{R} be the 'end-to-end' vector joining the two ends of the polymer, then

$$\mathbf{R} = \sum_{n=1}^N \mathbf{r}_n \quad (2.1)$$

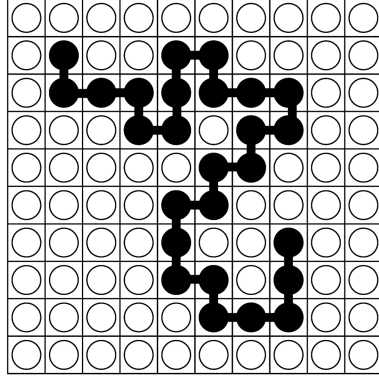


Figure 2.2: Random walk of a polymer chain on a two dimensional lattice [2]

where N is the number of bonds and \mathbf{r}_n is the vector of the n th bond. If we calculate the average of the square of \mathbf{R} , $\langle \mathbf{R}^2 \rangle$, since $\langle \mathbf{R} \rangle = 0$, we get the following expression from (2.1),

$$\langle \mathbf{R}^2 \rangle = \sum_{n=1}^N \sum_{m=1}^N \langle \mathbf{r}_n \cdot \mathbf{r}_m \rangle \quad (2.2)$$

However, since a single bond vector is independent of the direction of the other bond vectors, then eq. (2.2) holds only for $n = m$ and it turns out that,

$$\langle \mathbf{R}^2 \rangle = \sum_{n=1}^N \langle \mathbf{r}_n^2 \rangle = Na^2 \quad (2.3)$$

where a is the length of the bond in our lattice model. What we actually seek from this is the fact that the average value of the square of \mathbf{R} is proportional to N , thus if we take the square root of that we could clearly see that the size of the polymer, \mathbf{R} , is thereupon proportional to $N^{1/2}$. Let us from now on denote the end-to-end distance of an ideal free chain by $\mathbf{R}_o \sim aN^{1/2}$.

The probability distribution of the end-to-end distance is expressed by a Gaussian function,

$$P(\mathbf{R}, N) = \left(\frac{3}{2\pi N b^2} \right) \exp\left(-\frac{3\mathbf{R}^2}{2N b^2} \right) \quad (2.4)$$

It might be of interest to note that eq.(2.4) gives an expression for the entropy of the polymer chain at a fixed elongation [6] in 3 dimensions

$$\mathbf{S}(\mathbf{R}) = \mathbf{S}(0) - \frac{3}{2} k \frac{\mathbf{R}^2}{\mathbf{R}_o^2} \quad (2.5)$$

As the elongation (\mathbf{R}_o) increases, the entropy decreases. In terms of the free energy, eq.(2.5) becomes,

$$\mathbf{F} \simeq \frac{3}{2} kT \frac{\mathbf{R}^2}{\mathbf{R}_o^2} \simeq \frac{3}{2} kT \frac{\mathbf{R}^2}{N a^2} \quad (2.6)$$

If we derive the free energy with respect to the distance \mathbf{R} we get,

$$\frac{\partial \mathbf{F}}{\partial \mathbf{R}} = \frac{3kT}{N a^2} \mathbf{R} = \mathbf{f} \quad (2.7)$$

We can deduce that we have an entropic force \mathbf{f} acting on the chain to sustain its configuration with an end-to-end distance, \mathbf{R} . The expression of the force looks familiar and the coefficient can be seen as analogous to a spring constant. Thus, $3kT/(Na^2)$ plays the role of an entropic spring constant [12]. The lower the number of monomers N and the smaller the monomers (size a) are, the higher the "stiffness" of the chain. This fact is inversely true to the temperature T as well. It is also significant to note that the force increases as the chain is stretched, causing it to go back to a more probable configuration.

However, polymers are rarely ideal. If we inspect the ideal chain model carefully, we would realize that not only did we neglect any interactions between the chain and its medium and interactions between non-bonded monomers, we did not prevent

monomers from occupying the same space. The fact that two or more monomers can exist in the same space is in this case physically impossible, thus scientists were prompted to go further and investigate real polymer chains.

2.1.2 The Real Chain

For a more realistic approach, we must take into consideration long-range interactions between monomers along the chain as well as define an *excluded volume* that prohibits the overlap of monomers. Thus, instead of having a random walk, we are now dealing with a self-avoiding walk (SAW). When long-range interactions are taken into account, we will observe both attractive and hard-core repulsive forces in action. However, it is important to clarify that as an effective repulsive energy comes into play, the size of the real chain will become greater than that of an ideal chain, and it will be subject to the *swelling* of the chain. The *Flory theory* [4] of a polymer in a good solvent gives a beneficial evaluation of the free energy of a real chain, embracing both interactive and entropic contributions (explained in eq. 2.10). Let us assume that the swollen chain is of size R where $R > R_0 = aN^{1/2}$. P.J. Flory was aware that there is a cost in energy when we prevent a monomer in being within the excluded volume of another given monomer. The cost, which is known as the energy of excluded volume interaction, is (per monomer) [12],

$$F_{int\ per\ monomer} \approx kTv \frac{N}{R^3} \quad (2.8)$$

To get the energy for the whole chain, we need only to multiply eq.(2.8) by the number of monomers N and we get,

$$F_{int} \approx kTv \frac{N^2}{R^3} \quad (2.9)$$

where v is the excluded volume, and $R^3 \approx V$ with V being the volume occupied by the chain. We have so far discussed the interactive contributions involved in evaluating the total free energy F of the real chain. The entropic contribution, as estimated by Flory, is that associated with stretching an ideal chain to its end-to-end distance [eq.2.6], which has been discussed in Section (2.1.1) . Getting all the needed ingredients to calculate Flory's estimation of the total free energy, we arrive at the following,

$$F = F_{entropic} + F_{int} \approx kT \left(\frac{R^2}{Na^2} + v \frac{N^2}{R^3} \right) \quad (2.10)$$

At the beginning of this section, we assumed that our swollen chain has a size R different and greater than R_0 . To retrieve the expression of R , we take the minimum of the total free energy (i.e $\partial F / \partial R = 0$) expressed in eq.(2.10) . Thus the Flory theory produces R_F :

$$R_F \approx N^{3/5} a^{2/5} \quad (2.11)$$

It is important for the reader to appreciate the fact that the Flory theory delivers a universal power law concerning the dependence of the size R on the number of monomers in the chain N as follows,

$$R \sim N^\nu \quad (2.12)$$

where $\nu = 3/5$ (known as the scaling exponent) appears for swollen chains and $\nu = 1/2$ for ideal linear chains. However, later theoretical and experimental investigations have given a more accurate assessment for ν when it comes to 3 dimensional linear swollen chains [12]: $\nu = 0.588$.

2.1.3 Relaxation Times - A Harmonic Oscillator Approach

In order to understand the relaxation times of a real polymer chain, let us first take the example of the harmonic oscillator. The potential in this case is

$$U = \frac{1}{2} \kappa x^2 \quad (2.13)$$

(we take κ in order not to confuse it later on with k_B , the Boltzmann constant).

We can think of the stretching of the polymer to an un-equilibrium state as some displacement in the oscillator where they both tend to go back to some equilibrium state.

It is important to note that:

$$\langle x^2 \rangle = \frac{k_B T}{\kappa} \quad (2.14)$$

So, assuming x is similar to our polymer size R , in terms of κ we get:

$$\kappa = \frac{k_B T}{\langle R^2 \rangle} \simeq \frac{1}{N^{2\nu}} \simeq \frac{1}{N^{1.2}}, \quad \nu = 3/5 \quad (2.15)$$

The equation of motion of a harmonic oscillator is,

$$m\ddot{x} + \xi\dot{x} + \kappa x = 0 \quad (2.16)$$

Similarly, we can say that a polymer chain follows the same dynamics with $m = Nm_0$ where $m_0 = 1$ is the mass of the monomer and N is the number of monomers in the system. Whereas, $\xi = N\xi_0$ and ξ_0 is the coefficient of friction per monomer.

Dividing by m we get:

$$\ddot{x} + \frac{\xi}{m}\dot{x} + \frac{\kappa}{m}x = 0 \quad (2.17)$$

In order to check if our system is over-damped, critically damped or under-damped,

let us compare the relaxation time of the polymer with the period of “oscillations”.

Using dimensional analysis, we consider the following:

$$\frac{\xi}{m} = \frac{1}{T_{Rel}} \quad , \quad \frac{\kappa}{m} = \frac{1}{T_{(Osc.)}^2} \quad (2.18)$$

Then $\frac{T_{Rel}}{T_{(Osc.)}}$ becomes,

$$\frac{T_{Rel}}{T_{(Osc.)}} = \frac{\sqrt{m\kappa}}{\xi} \simeq \frac{\sqrt{NN^{-2\nu}}}{N} \simeq \frac{\sqrt{NN^{-1.2}}}{N} \sim \frac{1}{N^1} \sim N^{-1} \quad (2.19)$$

It is clear from eq. (2.19) that,

$$\frac{T_{Rel}}{T_{(Osc.)}} < 1 \quad T_{Rel} \ll T_{(Osc.)} \quad (2.20)$$

The above equation indicates that the relaxation time of the polymer in our system is much less than the period of oscillations. In turn, this proves that our system is an over-damped one. Following the analogy above, we can ignore the \ddot{x} term in eq.(2.17), and it becomes,

$$\dot{x} + \frac{\kappa}{\xi}x = 0 \quad (2.21)$$

with the following solution,

$$x \simeq \exp^{-\frac{\kappa}{\xi}t} \quad (2.22)$$

and the relaxation time τ being,

$$\tau = \frac{\xi}{\kappa} \simeq \frac{N}{N^{-2\nu}} \simeq NN^{2\nu} \simeq N^{2.2} \quad , \quad \nu = \frac{3}{5} \quad (2.23)$$

This indicates an existence of a power law between the relaxation times τ and the number of monomers N that goes like $N^{2.2}$. Now we know what to expect when solving and plotting for the τ vs. N .

2.2 The Locked Up Polymer Chain

Now that we have a better understanding of basic polymer characteristics and dynamics, we move a step closer to our main topic. Let us examine how a cylindrical confinement (with diameter D) affects the characteristics we have discussed so far. When brought under confinement, the spacial dimensions of a real chain are reduced at large scales. The Flory exponent (ν) changes accordingly [6],

$$\nu = \frac{3}{d+2} \quad \text{where } d \text{ is the dimensionality} \quad (2.24)$$

We've stated before that for a single free chain, the ideal chain radius is $R_0 \simeq N^{1/2}a$. For a free real chain we defined R_F where F stands for Flory. Let us redefine the latter into $R_{F_3} \simeq N^{\nu_3} \simeq N^{3/5}$ where 3 is for dimensionality. If we take this particular chain into confinement, its conformational behavior will alter. Considering that the confinement is a cylindrical pore with diameter D , we will have different regimes when comparing R_{F_3} to D .

If $D \gg R_{F_3}$ then we remain with $d=3$ and the chain acts as a free polymer in open space.

If $D \ll R_{F_3}$, the chain reveals one-dimensional behavior and a change in charac-

teristics. Let us now bring about the notion of *blobs*, where our polymer is divided into said blobs of diameter D . The number of monomers per blob is defined as,

$$g_D \simeq \left(\frac{D}{a}\right)^{1/\nu_3} \simeq \left(\frac{D}{a}\right)^{5/3} \quad (2.25)$$

The blobs act as hard spheres and display one-dimensional behavior. Now, the shape of the chain is outlined by a thickness D and a radius R_{F_1} given by,

$$R_{F_1} \simeq D \left(\frac{N}{g_D}\right)^{\nu_1} \quad (2.26)$$

Replacing g_D and ν_1 by their expressions we get,

$$R_{F_1} \simeq Na \left(\frac{a}{D}\right)^{2/3} \quad (2.27)$$

Now that we have the expression for the optimum size of a confined real chain, let us proceed and check what happens to the free energy of confinement.

$$F_{conf} \simeq Th(y) \quad \text{where } y = \frac{R_{F_3}}{D} \quad (2.28)$$

If the polymer acts as a free chain then there is no energy of confinement and,

$$h(y) = \begin{cases} 0 & \text{for } D \gg R_{F_3} \\ y^x & \text{for } D \ll R_{F_3} \end{cases} \quad (2.29)$$

Note that even though the chain acts with dimensionality 1 we have used R_{F_3} because this is the energy required to confine a free polymer chain of dimensionality 3.

$$F_{conf} \simeq k_B T \left(\frac{N^{3/5} a}{D} \right)^x \quad \text{for } D \ll R_{F_3} \quad (2.30)$$

We know that for $d = 1$ (blob picture), F should be linear in N and thus $x = 5/3$ and the free energy of confinement becomes as follows [5],

$$F_{conf} \simeq k_B T N \left(\frac{a}{D} \right)^{5/3} \quad (2.31)$$

Since polymer physicists are extremely fond of scaling laws, Burkhardt and Guim [13] have constructed a universal law for the relation between the energy of confinement and the average end-to-end distance of a confined chain in the scaling regime where $Na \gg D \gg a$:

$$\frac{F_{conf}}{R_{F_1}} = B \frac{k_B T}{D} \quad \text{and} \quad F_{conf} = B \frac{k_B T}{D} R_{F_1} \quad (2.32)$$

2.3 A Semi-Confined Polymer

Up until now (section 2.2), we have discussed a polymer entrapped in an infinitely long nanopore. In this chapter, we will study a semi-confined polymer chain along with its free energy of confinement and the entropic force acting on the confined part of the chain. To proceed, we cut the pore into a finite known length L , with a certain diameter D . The polymer will try to leave the pore and seek freedom. However, the means by which the polymer leaves the tube and the time required for it to do so is dependent on the size of the tail outside the pore. There exists a critical tail size N^* that defines two ejection regimes; $N > N^*$ and $N < N^*$. While both cases are equally important when it comes to ejection kinetics of polymer chains, we will focus on the long chains with tails ($N > N^*$). N^* is defined to be $L/a\lambda$, where λ is a strain parameter. In other words, and concerning blob sizes, we need the length of the tail to exceed the size of 1 blob with diameter equal to D . We have already acquired an expression for the free energy of confinement in an infinite pore, all we need to do in partial confinement is to consider the end-to-end distance of the confined part (ℓ) instead of R_{F_1} in eq.(2.32) [7]:

$$F = B \frac{k_B T}{D} \ell \quad (2.33)$$

It is well known that confining a flexible polymer chain inside a narrow tube leads to reduction in the configurational entropy and a corresponding increase in the free energy [6]. Studies by Klushin et al. [8] have also shown that the tail creates an entropically driven pulling force that acts on the confined part of the chain. It turned out that the force is independent of the size of the tail and can be understood as the slope of the free energy vs. the end-to-end distance of the confined part ℓ :

$$f = B \frac{k_B T}{D} \quad (2.34)$$

From eq.(2.34) we can deduce that the force is only dependent on the diameter and in fact, it decreases while increasing the diameter. The coefficient B that appears in eqs. (2.32, 2.33 and 2.34) is model-independent and is predicted to be 5.79 by Monte-Carlo simulations and renormalization-group theory [7]. It might be of importance to state that the dimensionality d ($d=3$ in our case), the monomer-tube interaction (repulsion, adsorption,...), the tube geometry (we have a circular tube), and the universality class of the monomer-monomer interaction (poor, good or θ -solvent) all affect the value of B .

Chapter 3

Molecular Dynamics Simulations

In the previous chapters, we have covered the foundations upon which our work is built, it is beneficial to try and illustrate in words how a Molecular Dynamics simulation works. MD simulations is at the heart of what we do and it is a tool that elegantly performs calculations we are incapable of carrying out analytically. It is a powerful procedure to compute equilibrium and dynamical properties of many-body systems [3]. If we look deep down into the backbone of this method, we would find that it integrates numerically the classical equations of motion to give us information about the positions and velocities of our atoms/monomers. Figure 3.1 is a flow diagram [14] illustrating a basic molecular dynamics algorithm:

3.1 Equations of Motion

To start with the basics of MD simulations, let us consider a system of N interacting molecules. We also assign to our system generalized coordinates and velocities, $\{q_i, \dot{q}_i\}$. Thus the Lagrangian $\mathcal{L} = \mathcal{L}(q_i, \dot{q}_i, t)$ of the system satisfies

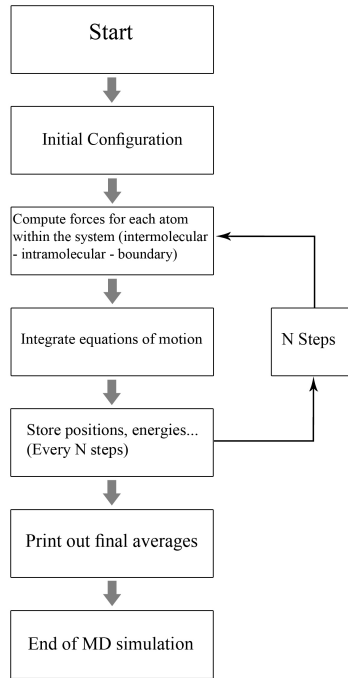


Figure 3.1: Diagram for an MD simulation algorithm [3]

$$\frac{d}{dt} \left(\frac{\partial \mathcal{L}}{\partial \dot{q}_i} \right) - \frac{\partial \mathcal{L}}{\partial q_i} = 0; \quad i = 1, 2, \dots, N \quad (3.1)$$

\mathcal{L} is defined by the potential and kinetic energies of the system. Ergo, if q_i connotes a component of the Cartesian coordinates for any of the atoms, and assuming the atoms have identical masses m we get [14],

$$\mathcal{L} = \frac{1}{2} m \sum_i \dot{q}_i^2 - U(\{q_i\}) \quad (3.2)$$

If f_i is considered the force corresponding to atom i then (3.1) is reduced to Newton's second law,

$$m\ddot{q}_i = -\frac{\partial U}{\partial q_i} = f_i \quad (3.3)$$

One of the most prominent properties of the classical equations of motion is the conservation law [3] . If our potential and kinetic energies are independent of time then our Hamiltonian H follows the same path, thus the change of H with respect to time is zero.

$$\dot{H} = \frac{dH}{dt} = 0 \quad (3.4)$$

where the Hamiltonian is defined as,

$$H(\mathbf{p}, \mathbf{q}) = \sum_k \dot{q}_k p_k - \mathcal{L} \quad (3.5)$$

In our simulations this is attained when all the forces acting on the system do not depend explicitly on time or velocities. Now to be able to solve the equations of motion we will have to integrate the 3N order differential equation i.e eq. (3.1). One should keep in mind that ultimately we do not want an exact solution. What we seek from a Molecular Dynamics simulation is to be able to envision thermodynamic properties and calculate time correlation functions that describe the dynamics of our system, as opposed to being able to track exact configurations of our atoms.

3.2 Verlet Methods

There exists more than one method to solve such a differential equation eq.(3.1). The Verlet Method which engulfs the "leapfrog" and velocity-Verlet algorithms is simple and time reversible. To acquire the Verlet equations we commence with a Taylor

expansion of the coordinate of the atom at $t + dt$ and $t - dt$, [15].

$$\mathbf{r}(t + dt) = \mathbf{r}(t) + \mathbf{v}(t)dt + \ddot{\mathbf{r}}\frac{dt^2}{2} + \dddot{\mathbf{r}}\frac{dt^3}{6} + \mathcal{O}(dt^4) \quad (3.6)$$

$$\mathbf{r}(t - dt) = \mathbf{r}(t) - \mathbf{v}(t)dt + \ddot{\mathbf{r}}\frac{dt^2}{2} - \dddot{\mathbf{r}}\frac{dt^3}{6} + \mathcal{O}(dt^4) \quad (3.7)$$

If we sum equations (3.6) and (3.7) we get the following,

$$\mathbf{r}(t + dt) = 2\mathbf{r}(t) - \mathbf{r}(t - dt) + \ddot{\mathbf{r}}(t)dt^2 + \mathcal{O}(dt^4) \quad (3.8)$$

where $\ddot{\mathbf{r}}(t) \approx \mathbf{f}_i$. The Verlet Method can be modified in two different ways, producing the "leapfrog" and velocity-verlet algorithms mentioned before. Our code employs the latter.

3.2.1 Velocity Verlet

Unlike the "leapfrog" algorithm where velocities and positions are not evaluated at the same time, velocity-Verlet (which from now on we will refer to as VV algorithm), allows us to compute both simultaneously. The VV algorithm adopts the previously mentioned Taylor expansion for computing the positions i.e eq.(3.6) including only second order derivatives and neglecting any higher order terms. Thus we get,

$$\mathbf{r}(t + dt) = \mathbf{r}(t) + \mathbf{v}(t)dt + \ddot{\mathbf{r}}(t)\frac{dt^2}{2} \quad (3.9)$$

By taking the time derivative of the preceding equation we get the desired velocities. Consequently we have,

$$\frac{d}{dt} \left[\mathbf{r}(t + dt) = \mathbf{r}(t) + \mathbf{v}(t)dt + \ddot{\mathbf{r}}(t)\frac{dt^2}{2} \right]$$

$$\mathbf{v}(t + dt) = \mathbf{v}(t) + [\ddot{\mathbf{r}}(t) + \ddot{\mathbf{r}}(t + dt)] \frac{dt}{2} \quad (3.10)$$

and in force notations our position and velocity equations come to be,

$$\mathbf{r}(t + dt) = \mathbf{r}(t) + \mathbf{v}(t)dt + \frac{1}{2m}\mathbf{f}_i(t)dt^2 \quad (3.11)$$

$$\mathbf{v}(t + dt) = \mathbf{v}(t) + \frac{1}{2m}[\mathbf{f}_i(t) + \mathbf{f}_i(t + dt)]dt \quad (3.12)$$

3.2.2 Numerical Scheme

1. Given initial positions \mathbf{r}_i and velocities \mathbf{v}_i , we compute all the forces acting on each atom/monomer
2. Use eq. (3.11) to update \mathbf{r}_i at $t+dt$
3. Since we do not have $\mathbf{f}_i(t + dt)$ we carry out a partial update for the velocities using $\mathbf{f}_i(t)$; let's call this a half-step at $\frac{1}{2}dt$:

$$\mathbf{v}_i(t + \frac{1}{2}dt) = \mathbf{v}_i(t) + \frac{\mathbf{f}_i}{2m}dt \quad (3.13)$$

4. Compute the new forces at $t+dt$
5. Having computed all the necessary components, we finally assess the velocities, $\mathbf{v}_i(t + dt)$
6. Repeat 1 \rightarrow 5

3.3 Forces

We have mentioned so far a force f_i acting on our monomer i . In this section we will explore the types of forces and their corresponding potentials that said atom experiences, leaving for later discussions the forces designed by our additional boundary conditions. If we consider our polymer to be free and experiencing a random walk, we are able to identify two types of interactions between our monomers: bonded and non-bonded interactions. Our potential energy function $U(\mathbf{r})$ is a combination of both.

3.3.1 Non-Bonded Interactions

Non-bonded interactions take place mainly between atoms of different molecules, or between atoms that are on the same molecule but are not chemically bonded. In other words, in our case, this interaction is between monomers of the same chain that are not considered to be "nearest neighbors" (adjacent monomers) and are at or smaller than a certain interactive distance from each other. The potential used in our simulations is the following [3]:

WCA Potential

The WCA potential is also known as the Weeks-Chandler-Anderson potential. It is mainly the repulsive part of the Lennard Jones potential and has a cutoff radius at the latter's minimum i.e. $r_{c(\text{WCA})} = 2^{1/6}\sigma_{LJ}$ and is shown to be,

$$U_{\text{WCA}}(r_{ij}) = \begin{cases} 4\epsilon \left[\left(\frac{\sigma}{r_{ij}} \right)^{12} - \left(\frac{\sigma}{r_{ij}} \right)^6 \right] + \epsilon & \text{for } r_{ij} < r_c = 2^{1/6}\sigma \\ 0 & \text{for } r_{ij} \geq r_c \end{cases} \quad (3.14)$$

3.3.2 Bonded Interactions

FENE Potential

Bonded interactions arise between atoms or monomers connected by chemical bonds [3], and their values mostly depend on the fluctuations of the chemical bond lengths and angles from equilibrium. In our system, we make use of the Kremer Grest potential. The KG potential is a combination of the FENE potential and the WCA. Assume our polymer is made of N monomers connected by an an-harmonic spring. All monomers including bonded ones interact with a repulsive Lennard Jones (WCA), and monomers that are nearest neighbors specifically interact by the Finite Extensible Nonlinear Elastic Potential. Thus the FENE contribution to the interaction due to two adjacent beads separated by \mathbf{r}_{ij} is,

$$U_{FENE}(r_{ij}) = \begin{cases} -\frac{1}{2}kR_o^2 \ln \left[1 - \left(\frac{r_{ij}}{R_o} \right)^2 \right] & \text{for } r_{ij} \leq R_o \\ \infty & \text{for } r_{ij} \geq R_o \end{cases} \quad (3.15)$$

where k is the spring constant for the FENE bond, and R_o is the limit of the bond extension.

Chapter 4

Our Own Adventure - The Road Taken

“It’s a dangerous business, Frodo, going out your door. You step onto the road, and if you don’t keep your feet, there’s no knowing where you might be swept off to.”

— J.R.R. Tolkien, *The Lord of the Rings*

It is convenient to remind the reader that we have made use of molecular dynamics simulations (check Ch. 3 for more details on how an MD simulation works) to study the dynamics origins of the entropic force of a partially confined polymer chain and the effects brought by the boundary shape and the length of the tail. We proceeded with adding the potential and the forces that arise from the walls of our tube. The force acts on individual monomers as a function of their positions and proximity to the walls. Afterwards, we move on to consider two limiting cases (discussed later on) concerning the semi-confined polymer chain.

4.1 Infinitely Long Pore

The first stepping stone we had to establish was to create the nanopore where we would be able to place the polymer. However, since we wanted to study the characteristics of a fully confined polymer chain as a first step, we start by constructing an infinitely long pore. In the simulations the wall is represented by a force acting on our monomers and inhibiting them from going outside. The walls are not permeable, rather they are purely repulsive. We should keep in mind that the force exerted should neither be too large so as to "throw" the monomer outside the tube, nor too small such that the monomer diffuses through the wall (in a one time step integration). One of the potentials that have the ability to exert such a force is the Lennard-Jones Potential. However, we only desire the repulsive part of the LJ potential (see fig. ??) which is also known to be the WCA potential mentioned in section 3.3.1.

The force exerted by the latter potential is that of the LJ potential; however we define a cutoff distance at $r_{ij} = 2^{1/6}\sigma$ that delivers a purely repulsive force.

$$F_{WCA/LJ} = \frac{24\epsilon}{\sigma} \left[2 \left(\frac{\sigma}{r_{ij}} \right)^{13} - \left(\frac{\sigma}{r_{ij}} \right)^7 \right] \quad (4.1)$$

The distance r_{ij} is between the monomer and a corresponding point at the walls of the pore. The function in the code responsible for calculating the force from the wall boundaries on the monomer takes r_{ij} as an argument, computes the force and implements it in the proper direction. The magnitude of the force in each direction (radially, no axial component) is then added to the net force acting on each monomer. When the latter is implemented in the velocity verlet process (section 3.2.1), we are left at each new time step (t) with new positions and velocities as an outcome of the forces at (t - dt).

Testing that the forces are working accordingly and the polymer is kept inside the pore,

we need only insert input variables analogous to the diameter and the length (infinite in this case) of the tube to run the simulations and extract the characteristics from the results obtained.

4.2 Assembling our Limiting Cases

Our main purpose was to inspect how different variables such as the diameter or the length of the tail of the polymer outside a semi-confined chain affect the results of studying the entropic forces acting on the confined part of the chain. Previously, in chapter 2, section 2.3 we discussed the thermodynamics background of the mentioned force. As of now, we are left with the molecular dynamics part of this story to be able to bring justice to the title of this thesis and finally compare the two.

I have stated earlier in this chapter that we consider two limiting cases here. The chain's environment now is made up of a cylindrical tube of length L (no longer infinite), with one end closed and the other open. The tube has an inner diameter D_{in} and an outer diameter D_{out} . Our two cases arise from the difference between the inner and outer diameter and are as follows,

4.2.1 Infinite Outer Boundaries

Here, the difference between both diameters is very large(see figure 4.1), and accordingly we can consider the flat edge surface at the open end of the tube to extend infinitely.

We have already constructed the inner tube along with its diameter D_{in} , we only need now to incorporate a method in the simulations which is analogous to an infinite wall at the boundaries. The easiest way is to take the exact same force used inside the tube in the radial directions and implement it at the flat wall in the axial direction

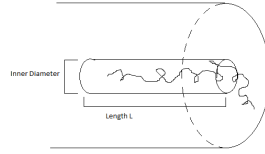


Figure 4.1: Sketch for a semi-confined polymer chain with infinite outer boundaries (large difference between D_{in} and D_{out})

only. So once a monomer is outside and close to the wall, it triggers a function in the simulation which calls for the WCA force to be evaluated. Thus, the particle will feel a "push" in the axially with a certain magnitude relative to its closeness to the boundary. Again, the force is purely repulsive, no adsorption or diffusion through the wall take place. However, the reader might ask, what is meant by too close to the wall. Since $\sigma = 1$ in the simulations, we have $r_m = 2^{1/6}\sigma$ where $r_m \sim 1.12246$ is the minimum distance needed between the wall and the the monomer before the latter feels any kind of force from the boundary (inter- and intra-molecular forces are not included in this force). At any other distance above that, the monomer experiences no repulsion from the wall. An input for an outer diameter D_{out} was not defined, we made the "virtual" wall extend in the yz -plane as far as the monomers tend to go.

4.2.2 Finite Outer Boundaries

In this second case, the difference between the diameters is very small and due to that, the polymer tail is free to access the space beyond the outer cylinder surface of the tube. All we have to do in the simulation is define a variable corresponding to the thickness of the boundary which substantially plays the role of the difference between

D_{out} and D_{in} . When the polymer chain's y and z positions flow beyond the second diameter, the chain is at liberty to explore all the free space around the nano-pore including the region close to the outer cylinder.

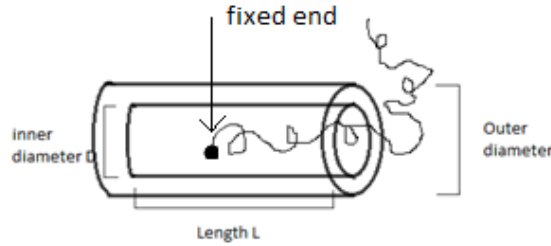


Figure 4.2: Sketch for a semi-confined polymer chain with finite outer boundaries (small difference between D_{in} and D_{out})

If it happens that the chain is too close to the outer cylindrical boundary of the tube, it experiences a repulsive force outwards and away from the boundary. All these forces are added to the total force acting on each monomer (i) and accounted for during the velocity verlet process.

4.2.3 The Inner and Outer Edges

As far as the edges are concerned, we assume that they are sharp corners. We use the WCA potential and define our cutoff to be at $2^{1/6}$. If the monomer lies anywhere between the length of the pore (L) and $L + cutoff$ axially and between the diameter D and $D - cutoff$ radially, then there exists a corresponding quarter circle with its center lying on the corner. Knowing the monomer's coordinates, we can calculate those of the circle affiliated to it where the latter has a radius of $2^{1/6}$. This process delineates the edges as curves rather than edges from the monomer's point of view.

4.3 Fixing the Polymer

We are almost done with the building blocks required to continue our research; however, we have yet one more task to formulate before we commence to collecting and analyzing results. If we mean to study the effects of the boundaries and the tail of the polymer on the entropic force, then we need the simulation to maintain a certain environment such that we take sufficient data points for analysis. We expect that during the simulation we always have collisions between the monomers and the outer boundaries and a certain length of the tail is somehow maintained. Thus, leaving the polymer to release itself from its constraints and allowing for a full ejection would not be very relevant to our studies. This leads us to setup our "apparatus" in such a way that the polymer is fixed inside the pore. Taking into account that we are using MD simulations and that there exists between the monomers of the same polymer inter and intra-molecular forces, we can simply try to fix the first monomer in space with a "harmonic oscillator". Nonetheless, we must make sure that the force exerted by the spring on the monomer is not high enough in magnitude to drag the polymer inside and not low enough to render the polymer outside leaving us with the initial concern. The reader should try and imagine that there is no actual spring attached to the monomer, only a force exerted in the axial direction (the force may be either positive or negative) that keeps the first monomer within a certain range(around 1-2 monomer size) from the origin. To implement this in our simulations, and to be able to use the same spring constant for all changing variables, we had to run some tests. We start initially with N monomers in an infinitely long pore with a given diameter D . We let the code generate new positions for the N monomers which are equally and horizontally placed on the x -axis. Since this is a highly improbable configuration, we run the simulation for some time such that we get a more reasonable structure. The polymer has now

diffused along the pore thus we shift the final coordinates produced in the initial run back to the origin along the x-axis only and we switch the harmonic oscillator on. By now we would have already defined an arbitrary value for the spring constant, given that said value is somehow reasonable (Some trial and error runs were made to get to a reasonable value). Currently, the first monomer should experience an axial force equal to $-kx$ where x is the distance from the origin (i.e the x coordinate of the first monomer). All we need to do now is to cut the infinite pore so that we are acquire a finite pore with length L . With a finite pore of length L , diameter D and fixed polymer we run the simulation again for a final time and obtain a file containing the magnitudes of the force felt by the first monomer. For statistical reasons, we go over the process several times to be able to get an average of the values we have. As a consequence, we now have several runs corresponding to different simulations ($\sim 2 \times 10^6$ iterations with an integration time step equal to 5×10^{-4}) stocked with the magnitude of the force from the spring. From these values we can create a histogram shown in fig.(4.3) and get an average of the force exerted on the fixed monomer.

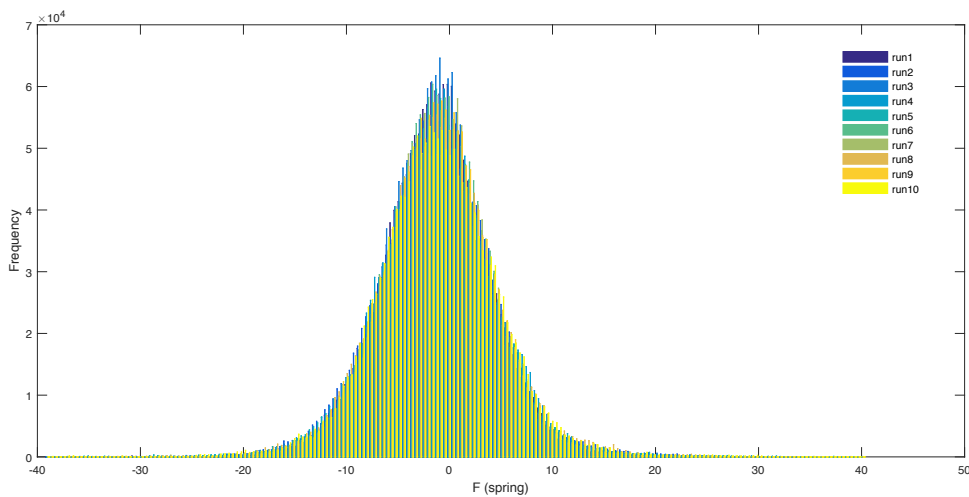


Figure 4.3: Histogram showing the frequency of the magnitudes of the force exerted by the spring on the fixed monomer

$$F = -kx \tag{4.2}$$

The average force turns out to be equal to -1.3425. Our aim is to find an ideal spring constant that only allows the first monomer to move 1 unit along the x direction from the origin, thus in eq. (4.2) we need x to be equal to 1. With that, we end up with a spring constant equal to 1.3425. We are currently almost at the top of the mountain. I would like to add a few more comments before we move on to the most important aspect of this thesis; the results.

4.4 Correlation Functions and Relaxation Times

In section 2.1.3 we discussed the notion of relaxation times of a free polymer chain and we are now aware of its dependence on the degree of polymerization N. As for a fully confined polymer chain we expect that the relaxation times would still depend on N; however, they would also rely on the diameter D in some way. The scaling law governing this dependence is,

$$\tau \sim N^2 D^{0.3} \tag{4.3}$$

As you can see, the dependence on N is weaker than that of a free polymer chain and we have an extra dependence on the diameter.

The code we have (original and added parts), does not calculate directly the relaxation times of the chain. However, it does calculate the correlation function, and from that we can determine the relaxation time τ . The correlation function, as the name implies, is the correlation of certain values of the system at different times or through the whole simulation time. The relaxation times in polymers as mentioned before can be

explained as the time it takes for the polymer to achieve an equilibrium state when it had started with a perturbed one. That is why the correlation function eq. (4.4) we have, calculates the association of the end-to-end distances of the chain throughout the process.

$$C(t) = \frac{\langle (R_{F_1}(t) - \langle R_{F_1} \rangle)(R_{F_1}(0) - \langle R_{F_1} \rangle) \rangle}{\langle R_{F_1}^2 \rangle - \langle R_{F_1} \rangle^2} \quad (4.4)$$

Taking the data obtained of the correlation function and plotting with respect to long-time behavior we get,

$$C(t) \sim e^{-t/\tau} \quad (4.5)$$

Thus, to get the relaxation time τ , after every simulation, we take the log-log plot of the correlation function versus time. The relaxation time τ is then $-1/slope$.

Chapter 5

Results and Analysis

It is of importance to state that throughout the whole simulations we used the WCA potential and force for non-bonded interactions and the KG potential and force for the bonded interactions between monomers. As for the mass (per monomer) and the temperature, we have $m = T = 1$. The maximum bond length of the FENE potential used in KG is $R_o = 1.5$ and its spring constant $k_{spring} = 30$. The friction coefficient used for the calculation of the total forces acting on the monomers and in the generation of the random noise component is $\gamma = 0.25$. The above parameters have these assigned values in most simulations unless otherwise is stated.

5.1 Free Polymer Chain

Before adding our new environment for the provided MD code, we commenced with some test runs to check the characteristics of a free polymer chain.

In figure (5.1) we see the dependence of the end-to-end distance of the polymer chain on the degree of polymerization N . The code calculates the end-to-end distances simply by getting the distance between the two end monomers of the chain; $R_{ee} =$

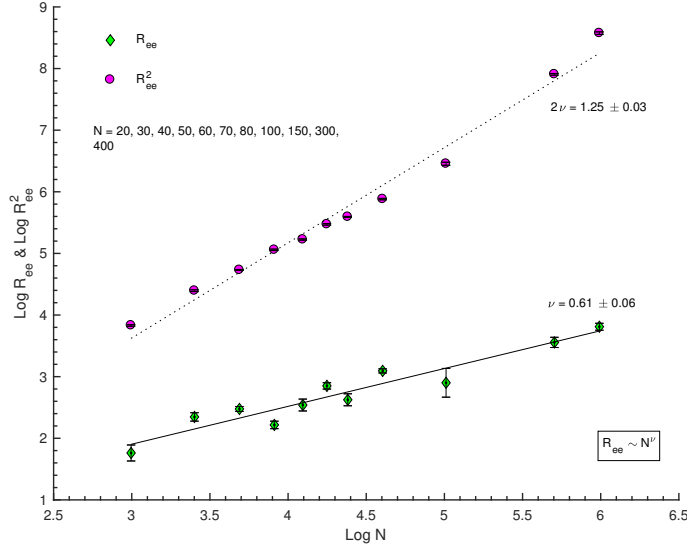


Figure 5.1: Plot of the end-to-end distances R_{ee} and R_{ee}^2 for a free polymer chain for different number of monomers N .

$\sqrt{(x_{end} - x_0)^2 + (y_{end} - y_0)^2 + (z_{end} - z_0)^2}$. From theory we know that $R_{ee} \sim N^\nu$ and $R_{ee}^2 \sim N^{2\nu}$ where ν is $3/5$ according to Flory and ~ 0.587 according to simulations. In fact, this is what we can see from our simulations as well. We have $\nu = 0.61 \pm 0.06$ where the error is that on the fit, and the error bars on the data points are standard deviations on the averages of the different runs for each N . We expect the dependence of the square of the end-to-end distance to be nothing but the square of ν and in fact, this is what we obtain.

Concerning relaxation times, the code only provides us (as stated before) with the time-dependent auto correlation functions eq.(4.4). However, we are able to get the relaxation times τ_{rel} by taking the log-log plots of $C(t)$ with respect to time and getting the slope of the linear part.

Our results of τ_{rel} vs. $N(\log - \log)$ agree with Eq. (2.23), where our simulations give $(2\nu + 1)$ to be 2.27 ± 0.08 .

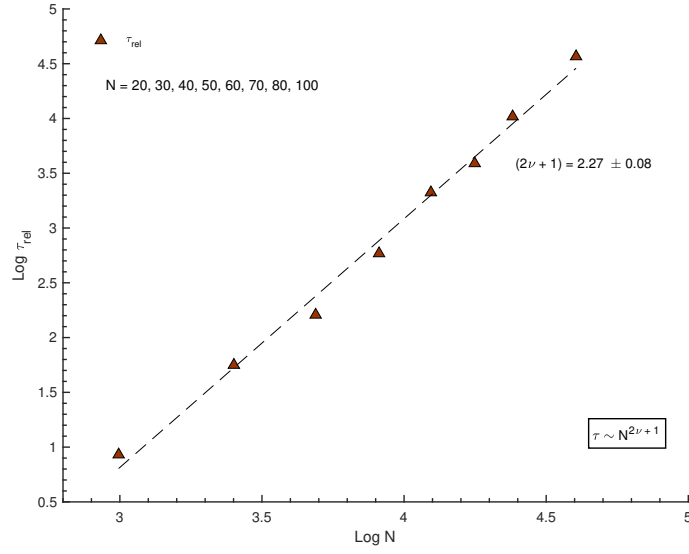


Figure 5.2: Plot of the relaxation times τ_{rel} for a free polymer chain for different number of monomers N .

5.2 The Fully Confined Polymer Chain

5.2.1 Average chain size characteristics

According to the blob picture, (refer to section 2.2), a polymer chain in a cylindrical confinement acts as a one dimensional self-avoiding walk with a certain number of blobs n_b each of size D (diameter). Scaling theories predict the average end-to-end distance to be (with $\nu \sim 3/5$),

$$R_{F_1} \sim n_b D \sim ND^{1-1/\nu} \sim ND^{-2/3} \quad (5.1)$$

Fig. (5.3a) and (5.3b) present the average lateral component of the end-to-end distance (and R_{ee}^2), which we define in eq. (5.1) to be R_{F_1} versus the degree of polymerization N . The two fits give us on average a power law dependence of (1.15 ± 0.06) and (2.32 ± 0.06) for R_{ee} and R_{ee}^2 respectively. For the fully confined chain, in com-

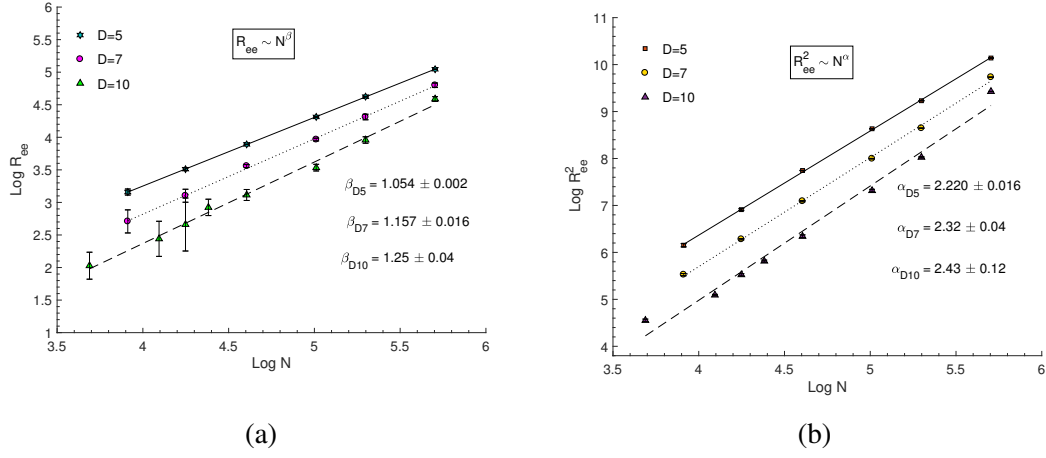


Figure 5.3: Power law governing R_{ee} (a) and R_{ee}^2 (b) dependence on N .

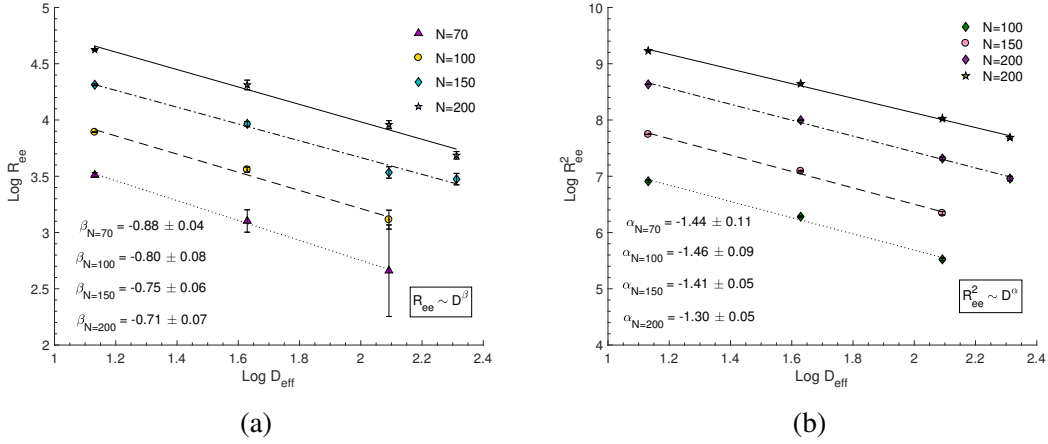


Figure 5.4: Power law governing R_{ee} (a) and R_{ee}^2 (b) dependence on D .

parison with the free chain, we have an extra dependence of the end-to-end distance on the diameter D . However, we must note that for all fits concerning the diameter (including semi-confinement), we found out that there exists a nonuniversal correction to the pore's diameter D to $D - \delta$, which we will call the new effective diameter, with $\delta = 1.9$.

Figures (5.4) and (5.3) produce the following scaling arguments,

$$R_{ee} \sim CN^{1.1}D_{eff}^{-0.78} \quad (5.2)$$

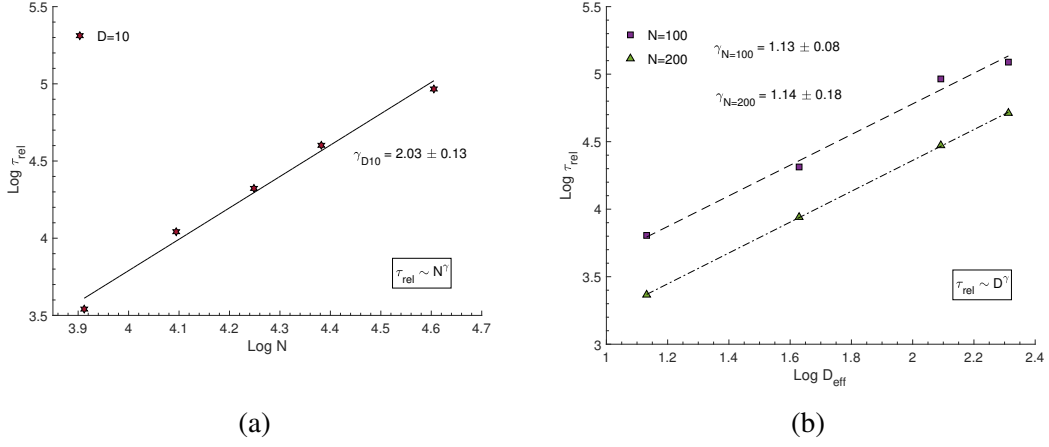


Figure 5.5: (a) shows the dependence of the relaxation times on N . (b) shows the dependence of the relaxation times on the effective diameter.

where our simulations show that $R_{ee} \sim D_{eff}^\alpha$ with $\alpha = -0.78 \pm 0.04$ and $R_{ee}^2 \sim D_{eff}^{2\alpha}$ with $2\alpha = 1.4 \pm 0.03$. The model-dependent numerical prefactor, C , in eq. (5.2) has been estimated in two ways and turns out to have the following values,

$$C = \begin{cases} 1.11 \pm 0.08 & \text{from y-intercept of } \log(D_{eff}) \text{ vs. } \log(R_{ee}) \\ 1.20 \pm 0.04 & \text{from plot of } R_{ee} \text{ vs. } ND^\alpha \end{cases} \quad (5.3)$$

5.2.2 Relaxation time measurements

Now we attend to the global relaxation times τ_{rel} of a confined polymer chain. For weak confinements, we know that the behavior of the relaxation times falls back to the scaling behavior of a free polymer. When strong confinement is concerned, we expect the scaling result to go like $\tau_{rel} \sim N^2 D^{2-1/\nu} \sim N^2 D^{0.3}$. Using the slowest exponential decay of the autocorrelation function, the relaxation times we find in our MD simulation scale approximately as (check fig. (5.5)),

$$\tau_{rel} \sim N^{2.03} D^{1.14} \quad (5.4)$$

This results shows an agreement in the dependence on N; however, it demonstrates a much stronger dependence on D. Relaxation times are associated with large scale microscopic motion of the polymer chain. This type of motion can be affected by the elastic characteristics of the chain and its surroundings. Other MD simulations by Arnold et al. [11], show a lower dependence on N and a higher on D, with their relaxation times going as $\tau \sim N^{1.75}D^{1.3}$. However, they were able through their Monte Carlo simulations to consider higher degrees of polymerization N and ended with the same dependence on N yet with a slightly weaker dependence on D and in more agreement with the theory ($\sim D^{0.75}$). This implies that it is possible for us to obtain a scaling law close to the theory if we are able to go further into strong confinement with higher N, especially concerning the dependence on D. It is not possible for us to go to lower diameters, because then the pore would be too narrow, considering the effective diameter, ($D_{eff} \simeq \text{size of monomer}$) and it would be almost impossible for two monomers to move both radially and axially.

5.2.3 Free energy and force

A chain confined in a cylindrical pore consists of n_b blobs each of size D. Each blob contains a certain number of monomers $g = (D/a)^{1/\nu}$ dependent on the diameter, which result in a total number of blobs $n_b = N/g \sim ND^{-1/\nu}$. The free energy of confinement (in units of $k_B T$) is,

$$F_{conf} = An_b = AND^{-1/\nu} = AND^{-5/3} \quad (5.5)$$

A, similarly to C in R_{ee} , is dimensionless and a model-dependent numerical coefficient. MD simulations do not directly calculate the energy, but we can get the radial force acting on the wall. From our simulations, we need only to take the sum of the

magnitude of the radial forces acting on each monomer at each time step and average over all time-steps to get an average of f_{radial} . The radial components of the force at each time step and on average add to up zero, thus we only use the magnitudes. From the confinement free energy, f_{radial} is simply derived;

$$f_{radial} = -\frac{\partial F_{conf}}{\partial r} = 2\frac{\partial F_{conf}}{\partial D} = \frac{2A}{v}ND_{eff}^{-1/v-1} \quad (5.6)$$

where $(-1/v - 1) \sim -2.67$.

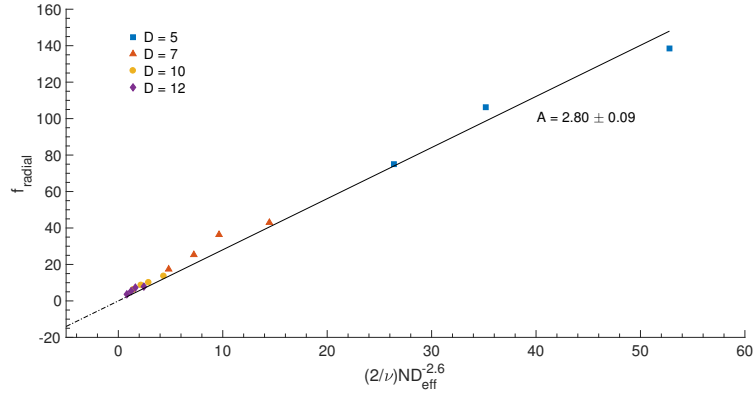


Figure 5.6: Variation of f_{radial} with the scaling variable $(2/v)ND_{eff}^{-2.6}$

Figure (5.6) shows the radial force plot versus the scaling variable $(2/v)ND_{eff}^{-2.6}$. The coefficient A from this plot is equivalent to $A = 2.80 \pm 0.09$. Even though we are aware that A is model-dependent and there is no universal value governing it, we know that a combination of A and C (A/C), produces a model-independent universal prefactor B. For this reason, we go on to check the validity of the scaling argument we used with our MD simulations. First, we check the dependence of f_{radial} on D, and it turns out that $f_{radial} \sim D_{eff}^{\beta}$ where $\beta = -2.32 \pm 0.04$ instead of -2.67 . Using the same plot ($\log(D_{eff})$ vs $\log(f_{radial})$) we are able to deduce the value of A from the y-intercept where,

$$A = \frac{\mathbf{v}e^{y-int.}}{2N} \quad (5.7)$$

which results in $A = 2.14 \pm 0.04$. This result is fairly similar to what we produced before. It is prominent that eq. (5.7) depends still on only one variable; N. Examining the power law governing f_{radial} and N, we find out that according to our MD simulations, f_{radial} is not linear in N, in fact, $f_{radial} \sim N^\lambda$ where $\lambda = 0.78 \pm 0.04$. Checking again with eq. (5.7) but with our new N dependence, we get $A = 6.45 \pm 0.46$. Now that we know how f_{radial} acts like in terms on D_{eff} and N according to our MD simulations, we can temporarily change eq. (5.6) to be,

$$f_{radial} = \frac{2A}{\mathbf{v}} N^{0.78} D_{eff}^{-2.3} \quad (5.8)$$

Plotting f_{radial} with the new scaling argument we get $A = 6.13 \pm 0.14$.

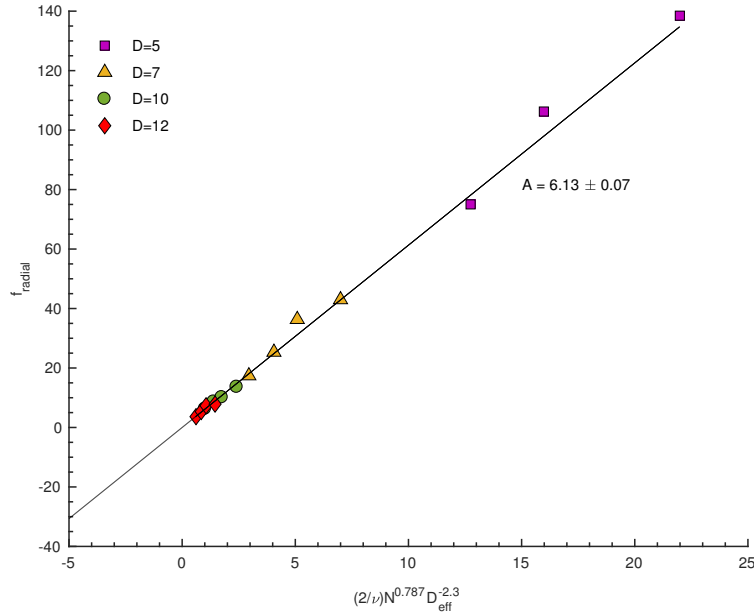


Figure 5.7: Variation of f_{radial} with the scaling variable $(2/v)N^{0.78}D_{eff}^{-2.3}$

Taking the ratio of the radial force and the end-to-end distance we get,

$$\frac{f_{radial}}{R_{ee}} = \frac{2}{v}BN^{-0.22}D^{-1.7} \quad (5.9)$$

where $B = A/C = 5.79$ as stated before, is a model independent universal constant.

From our simulation we can now deduce B in three different approaches.

1. Ratio of A and C evaluated from the y-intercepts of $\log(D_{eff})$ vs. $\log(f_{rad})$ and $\log(D_{eff})$ vs $\log(R_{ee})$ respectively
2. Ratio of A and C evaluated from the slopes of f_{radial} vs. $(2/v)N^{0.78}D^{-2.3}$ and R_{ee} vs. $ND^{-0.7}$ respectively
3. Get B directly from the plot of $\frac{f_{radial}}{R_{ee}}$ vs. $(2/v)N^{-0.22}D^{-1.7}$

From equations (5.3) and (5.7), we have ($B = 5.8 \pm 0.58$) for case(1). For case(2) we have $B = 5.11 \pm 0.2$. As for case(3), fig. (5.8) shows the value of B, for $N = 150, 200, 300$, to be $B = 6.6 \pm 0.2$.

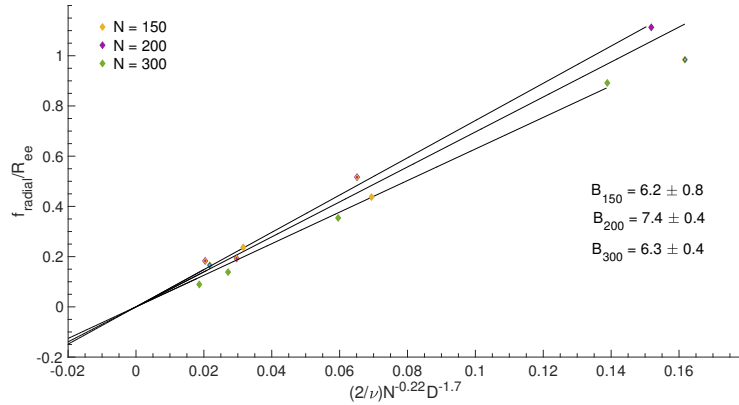


Figure 5.8: Variation of f_{radial}/R_{ee} with $(2/v)N^{-0.22}D^{-1.7}$ produces the constant B.

From our values of the end-to-end distances and the radial force, we can conclude that we do not reach the asymptotic limits stated by the theory concerning the de-

dependencies on N and D . The dependence on the diameter is different and we can still observe a dependence on N . Therefore, concerning the value of B in this case, it might not be significant to compare it to the universal constant and discuss the discrepancies we have.

5.3 The Semi-Confined Polymer Chain

As the reader might know by now, our main concern in this research is to study the dynamic origins of the entropic force generated when a polymer chain is put into semi-confinement. The source of the entropic force is the difference between the free energies outside and inside. Since the free energy outside is less than that of the confined part, the polymer chain tends to go outside, resulting in this entropic force acting on the confined part. In an MD method, we are unable to calculate entropies and energies directly, thus we try to mimic the entropic force by a pulling force produced by our potential at the walls. To understand this force more, we take a look at the free energy of the confined part.

Since we have our polymer fixed inside the tube, then the distance from the inner chain end to the tube's opening is simply the length of the pore L .

$$F = B \frac{k_B T}{D_{eff}} L \quad (5.10)$$

The force is consequently,

$$f = B \frac{k_B T}{D} \quad (5.11)$$

Initially we need to check that the magnitudes of the pulling force is in fact the same for the two limiting cases. The first step we did was to check that the dynamics

Table 5.1: Pulling Force (Infinite Boundaries)

Pulling Force (Infinite Boundary)				
Diameter	5	7	10	12
Number of monomers N	N = 150, 200, 300	N = 150, 200, 300	N = 150, 200, 300	N = 150, 200, 300
Pulling Force	1.054 +/- 0.006	0.645 +/- 0.008	0.386 +/- 0.005	0.299 +/- 0.002

Table 5.2: Pulling Force (Finite Boundaries)

Pulling Force (Finite Boundary)				
Diameter	5	7	10	12
Number of monomers N	N = 150, 200, 300	N = 150, 200, 300	N = 150, 200, 300	N = 150, 200, 300
Pulling Force	1.036 +/- 0.002	0.66 +/- 0.02	0.42 +/- 0.02	0.32 +/- 0.01

are working properly each time we ran a simulation. At the end of each simulation, we were presented with the total forces acting on the whole system. This total force consists of the average inter and intra molecular interactions, the force from the spring keeping our polymer in place, the radial forces inside the tube and the forces produced from the outer boundaries. The last force encompasses the force from the inner edge and the flat outer wall for the infinite boundary case, and the force from the inner and outer edge as well as the wall with thickness h for the finite boundary case. We also made sure that the total force is negligible and that the average position of the center of mass of the polymer chain is stationary which results in no type of diffusion inside or outside the pore.

5.3.1 Pulling Force

From eq. (5.11) we clearly see that the force is independent of the number of monomers in the system, and in fact this is what our simulations show. Thus we are able to present tables (5.1) and (5.2) of the pulling force as a function of D averaged over several runs for different values of N .

If one ignores the theoretical predictions concerning these two cases, one would think that in a dynamical setting such as ours it seems logical that the frequency of collisions with the wall in the case of the infinite boundary should be greater than that in the case of finite boundaries. This reasoning leads to another assumption that there should be a significant difference in the magnitude of the pulling force in the two cases. However, the simulations clearly agree with the theoretical predictions that suggest that both forces boil down to the same expression and dependencies in eq. (5.11) .

One of these dependencies is that of the diameter D . We know that $f_{pull} \sim D_{eff}^{-1}$.

Figure (5.9) shows the dependence of the pulling force on the diameter for finite outer boundaries $f_{pull} \sim D^\mu$ where $\mu = -1.057 \pm 0.007$. As for the infinite boundaries figure (5.10) result in $\mu = -1.060 \pm 0.006$. One way to explain this similarity between the two cases is to consider that eventhough the finite boundary has less area for collisions, the fact that there is free space beyond the boundary allows the chain to get closer to the wall creating new interactions or generates higher magnitudes. This topic will be discussed later, thus for now we move to check how the pulling force is affected by the change in temperature.

We expect a rise in the pulling force in association with the increase of the system's temperature. The system's temperature is kept constant using a Langevin thermostat; however, with a temperature increase the molecules' velocities are higher, thus if a monomer is approaching the wall with temperature $T_2 > T_1$ for a certain time-step it will approach with higher velocity. The latter leaves the monomer closer to the wall and in turn creates a higher repulsive force resulting in a higher pulling force. The opposite also applies for cases where $T_2 < T_1$. (Assuming T_1 is what we have worked with up till now with $T = 1$).

Fig. (5.11) shows that if $f_{pull} \sim T^\phi$ then $\phi = 0.92 \pm 0.02$, and table (5.3) shows

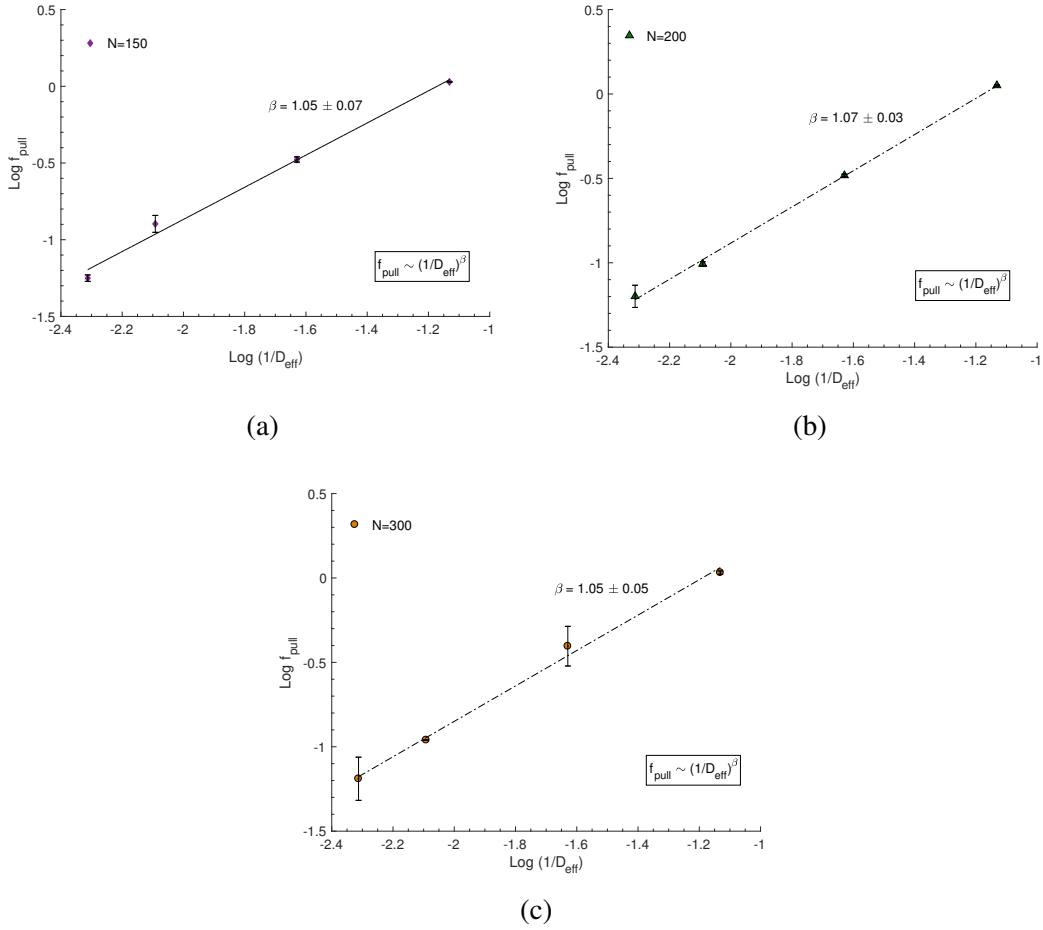
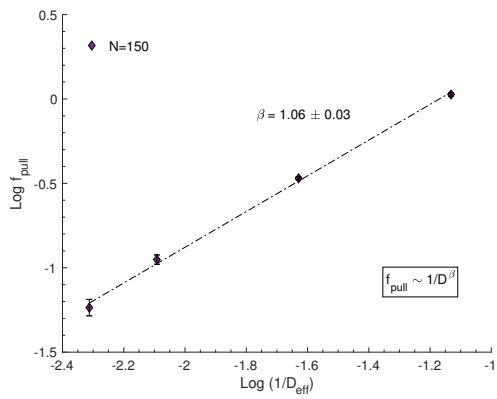


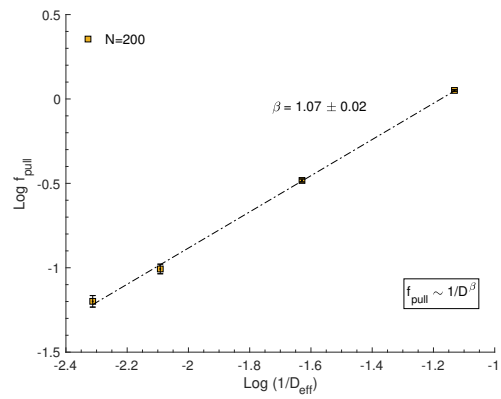
Figure 5.9: Finite Boundary: The dependence of f_{pull} on D_{eff} for $N = 150, 200, 300$ in (a) , (b), and (c) respectively.

Table 5.3: Pulling Force dependence on T

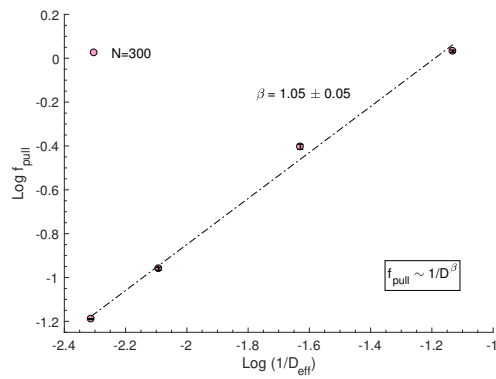
Dependence of pulling force on T					
Diameter = 5					
Temperature	0.5	1	2	5	7
Pulling Force	0.723 +/- 0.009	1.03465 +/- 0.007	2.51 +/- 0.05	5.75 +/- 0.01	7.86 +/- 0.02



(a)



(b)



(c)

Figure 5.10: Infinite Boundary: The dependence of f_{pull} on D_{eff} for $N = 150, 200, 300$ in (a), (b), and (c) respectively.

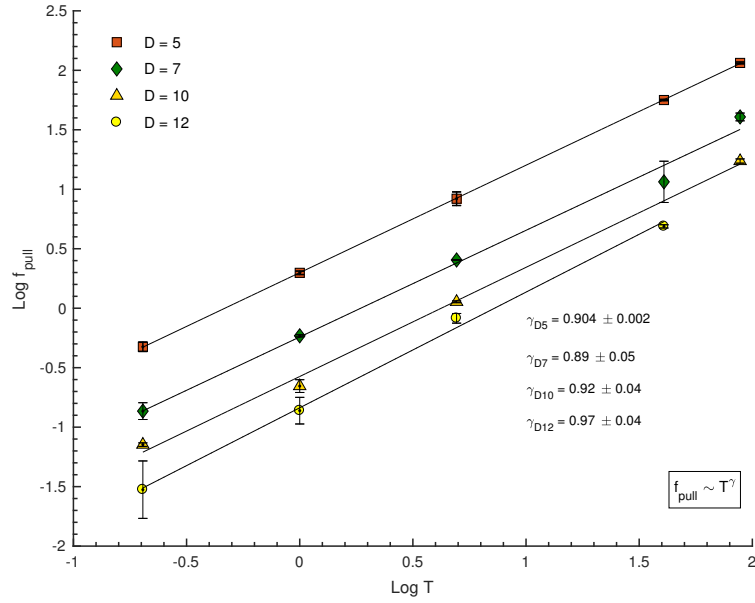
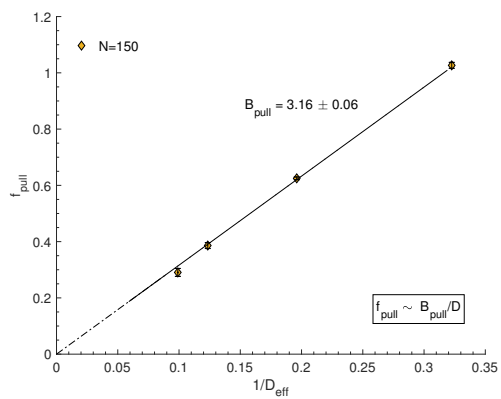


Figure 5.11: The dependence of the pulling force on the temperature T for $T = 1/2, 1, 2, 5, 7$.

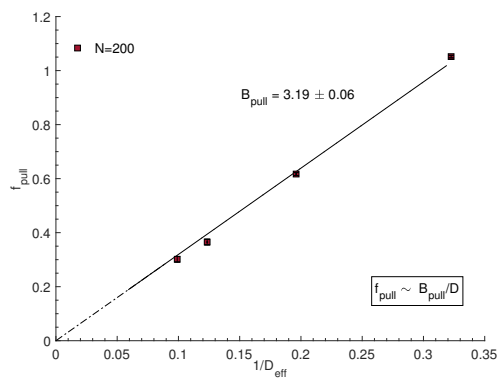
numerical results for $D = 5$. It occurs that for a semi-confined chain, unlike the full confinement case, we are able to reach, in f_{pull} , the asymptotic limits in T and D . We do not find any dependencies on N and that of D is as expected thus we are able to proceed with extracting the coefficient B .

For the infinite boundary case, ($T = 1$) we can see from fig. (5.12) that a plot of f_{pull} against $1/D_{eff}$ yields $B = 3.19 \pm 0.02$ while for the finite boundaries we produce fig. (5.13) whose results concur with those of an infinite boundary with $B = 3.30 \pm 0.04$.

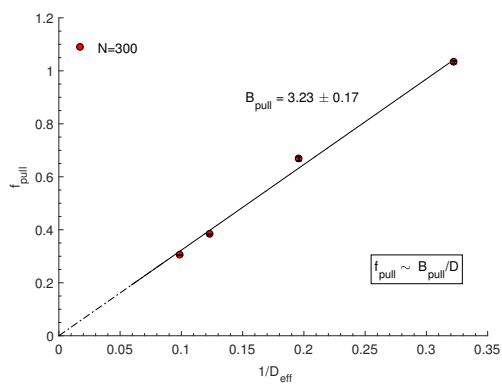
Up till now, we have assumed that the coefficient B in eq. (5.11) is the same as that for a fully confined chain. However, that may not be the case, and the fact that B is a model-independent universal constant might not be true in the case of semi-confined chains under the effect of a pulling force.



(a)

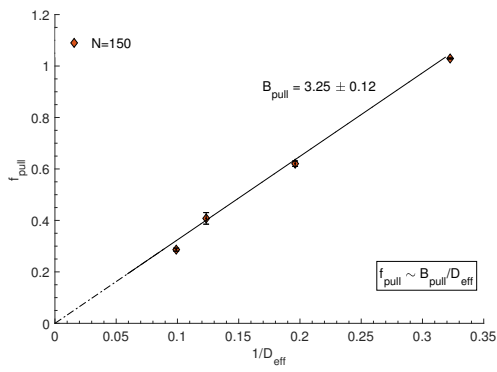


(b)

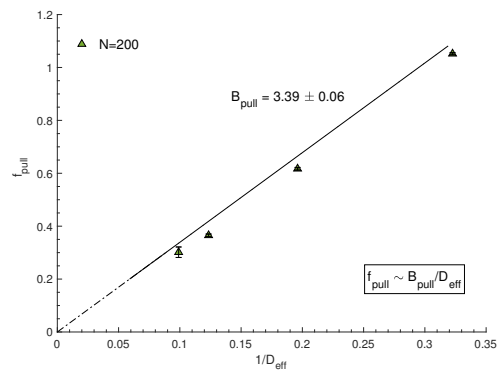


(c)

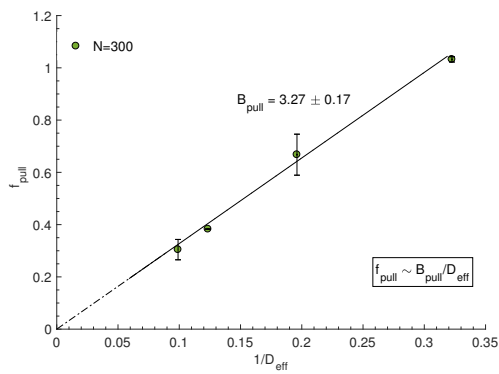
Figure 5.12: For infinite boundaries and for different values of N , we plot f_{pull} against $1/D_{eff}$ to extract the coefficient B



(a)



(b)



(c)

Figure 5.13: For finite boundaries and for different values of N , we plot f_{pull} against $1/D_{eff}$ to extract the coefficient B

5.3.2 Radial Force

If $f_{pull} = \frac{\partial F}{\partial L}$, then as in the case of full confinement, $f_{radial} = 2\frac{\partial F}{\partial D}$.

$$f_{radial} = \frac{2BL}{D^2} = \frac{2Lf_{pull}}{D} \quad (5.12)$$

If we start with the first equality in eq. (5.12) we can extract, using another method, the coefficient B and check if it is consistent with the results we obtained before.

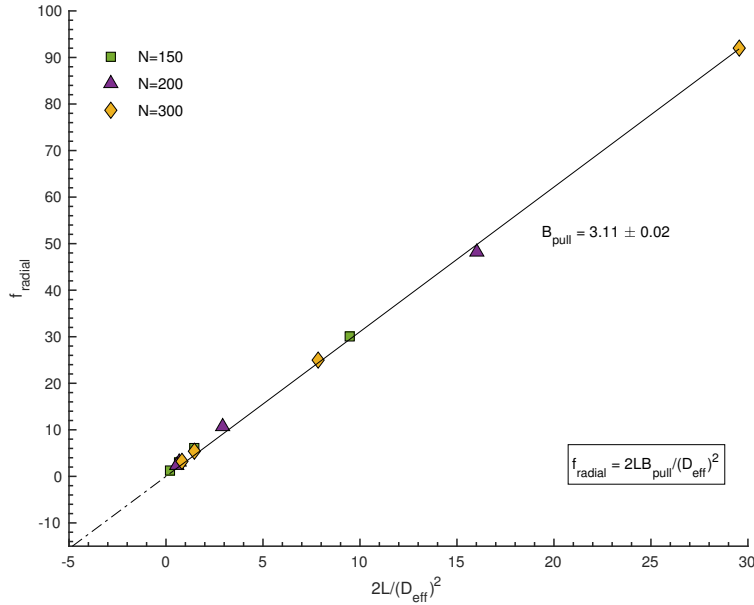


Figure 5.14: Plot of f_{radial} against $\frac{2L}{D^2}$ for a semi-confined chain produces the coefficient B.

In agreement with our previous results, fig. (5.14) gives $B = 3.11 \pm 0.02$, thus from now on we will call the coefficient derived from the pulling force \tilde{B} instead of B. However, before we state whether the theoretical prediction about B is true for a case like ours, let us proceed with another testing method.

5.3.3 Confined Pull

To be able to study both \tilde{B} and B simultaneously we go back to the case of a fully confined chain. We keep the chain connected to the spring keeping it in place and we apply a force to the other end. The final magnitude of the force is equal to the average pulling force in the semi-confined case in terms of the diameter D .

We start with a given number of monomers N and diameter D in a confined tube. We start with a zero magnitude pulling force and start increasing it until we get to a maximum of f_{pullD} . Simultaneously, we would be recording the force felt by the spring and the changes in lengths at certain timesteps and increments of the force. Thus now we have the change in length with respect to the force $l(f_{pull})$. We run for each increment long enough such that we get to an equilibrium length before altering the magnitude. If F is the total free energy of the system, we can write it as follows,

$$F_{total} = F_0 + F_1 \quad (5.13)$$

where F_0 is the free energy only due to confinement and F_1 is that due to the pulling force. The final length of the chain is,

$$l = l_0(1 + \varepsilon) \quad (5.14)$$

where $\varepsilon = \Delta l / l_0$. Dividing the free energy by the length we get,

$$\frac{F}{L} = \frac{F_0 + F_1}{l_0(1 + \varepsilon)} \quad (5.15)$$

Replacing F/l by the force f , which is the force felt by the spring, and $F_1 = Bl_0/D$,

Table 5.4: Data for Confined Pull

N / Diameter	f(pulling)	Free Energy	B (confinement)
N = 200 / D = 5	1.045	113.96	5.58
N = 150 / D = 5	1.045	85.8009	5.233
N = 200 / D = 7	0.64	51.2903	5.397
N = 200 / D = 10	0.4	27.5636	5.25
N = 150 / D = 10	0.4	21.4527	5.237

$$f(1 + \varepsilon) = \frac{B}{D} + \frac{F_1}{l_0} \quad (5.16)$$

All the needed measurements are provided by the simulations and we apply a simple trapezoidal method of integration on $l(f)$ vs. f to obtain $F_1 = \int f dl$. For a specific N and D , we use eq. (5.16) to get B and we are also capable of deducing \tilde{B} from $F_1 = \tilde{B}l_f/D_{eff}$. If the values we obtain for B are in agreement with the theory, then we know that all the asymptotic limits we discussed before have been reached and then it would be valid for us to extract the value for \tilde{B} then compare with its previous values in sections (5.3.2) and (5.3.1), with B and comment on the results.

Table (5.4) shows that $B = 5.34 \pm 0.07$ compared to the theoretical value of 5.79. Proceeding with the calculations of \tilde{B} , from F_1 we obtain $\tilde{B} = 3.1 \pm 0.2$ which is consistent with the previous two results. It is clear that the free energy of confinement in an infinite tube is different from the free energy of confinement of a chain in semi confinement under the effect of a pulling force. Eventhough R_{ee} switches to L (length of pore) in semiconfinement, the amplitudes B and \tilde{B} in turn are also modified. Thus it is safe to say that the model-independent universal constant B , is so for fully confined chains in a tube; however this does not apply in our model. To explain this discrepancy between the two constants related to the free energies of fully and semi-confined chains, we think of the free energy of full confinement as F_0 and that

Table 5.5: Data for radial force and pulling force for N=300 for semi-confined chain

N = 300				
D (diameter)	L (length of pore)	F _{radial} (simulation)	F _{pull} (simulation)	F _{pull} (calculated)
5	142.25	92.0	1.032	1.0043
7	102	24.9	0.667	0.6244
10	47.7	5.4	0.382	0.4556
12	42	3.22	0.304	0.3874

of semi-confinement as $F_0 + \Delta W$. ΔW is the work done by the pulling force in both semi-confinement and the confined pull method. The free energy per monomer shows that $F_0/N < (F_0 + \Delta W)/N$ for the same number of monomers N. However, when taking the free energy per unit length, which is equal to the force we are calculating, $F_0/L_1 > (F_0 + \Delta W)/L_2$ where L_1 is the length of a relaxed polymer chain and L_2 is that of a stretched chain due to a pulling force resulting in $L_2 > L_1$. From this we can deduce that the free energy in a fully confined state is less than the free energy of a polymer chain in semi-confinement; however, the difference between the free energy per unit length discussed above results in the difference between the coefficients \tilde{B} and B.

5.3.4 Relation between radial and pulling force

Following from eq. (5.12), we possess a correlation between the pulling force f_{pull} and the radial force f_{radial} for a chain in semi confinement. Plotting f_{radial} against $f_{pull}L/D_{eff}$, we get a slope of magnitude 2 as seen in fig.(5.15).

Assuming we do not have the values for the pulling force, we can extract them and compare to previously obtained values.

Table (5.5) shows the pulling force obtained from the simulations and the calculated values for $N = 300$ and $D = 5, 7, 10, 12$.

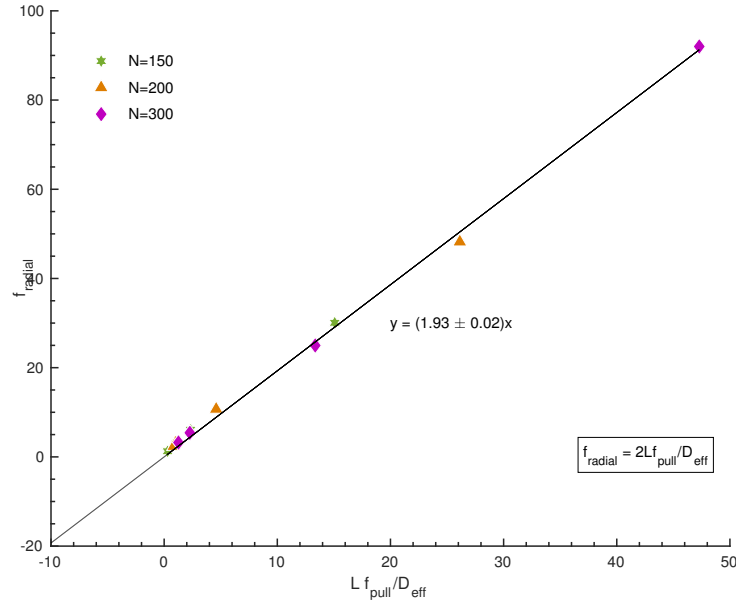


Figure 5.15: Plot of f_{radial} against f_{pull} for a semi-confined chain.

5.3.5 Effects of the tail

A study, by Klushin et al. [8] investigated the dragging of a polymer chain inside a nanotube. The study defines the end monomer position inside the tube to be x , and they show that there exists a critical value for x called x^* . Relying on theory and MC simulations, they prove that if the ratio of $\frac{x}{x^*} > 1$, that is if the length of the polymer inside the tube exceeds the critical length, the partial confinement is not longer an equilibrium state and the chain is dragged inside and the free energy becomes that of total imprisonment. If $\frac{x}{x^*} < 1$, then the chain is in what is known to be as a partially confined "flower" state and the amplitude of the free energy, in affinity with out results, is no longer the universal constant $B \sim 5.79$ but defined to be,

$$F_{fl} = 4.27x/D \quad (5.17)$$

There is a discrepancy between the value of \tilde{B} in eq.(5.17) and ours. This mismatch may be due to the fact that the study uses Monte Carlo simulations and were able to extract the value from values of the free energy. The parameter x is fixed in our case and known to be L (the length of the tube). If we come to think about this in reverse, then if there exists a length of the polymer inside the tube above which the chain is drawn inside, then there most certainly exists a length outside below which the same process also occurs and that length is known to be greater than a blob size.

In this section, instead of checking free energies, we will check whether the polymer will experience a pulling force as we decrease the number of blobs outside the tube until the tail is smaller than a blob, and whether the chain will be lured inside or keep its partially confined state.

In our code, L is calculated by using the input values of the diameter and the number of blobs desired outside. We administered the runs for $N = 150$ and $D = 7$, and in fig.(5.16) we can see that we get the same magnitude for the force even when the size of the tail outside is less than 1 blob. The final configurations also show that the polymer still has a tail outside and did not switch to full confinement.

$$L^* = 1.265 \frac{N}{D^{1-1/\nu}} \quad (5.18)$$

To write L^* in terms of the number of blobs, multiply and divide eq.(5.18) [8] by $D^{1/\nu}$ and take $N/D^{1/\nu}$ to be the number of blobs, we get

$$L^* = 1.265 D^{-0.2} n_b \quad (5.19)$$

Thus for $N = 150$ and $D = 5$, $L^* = 0.913 n_b$.

The last two columns of table(5.6) yield the ratio $L/L^* = 1.02 > 1$ and $1.06 > 1$, yet we still remain in the semi-confined state. However, it should be stated that n_b is

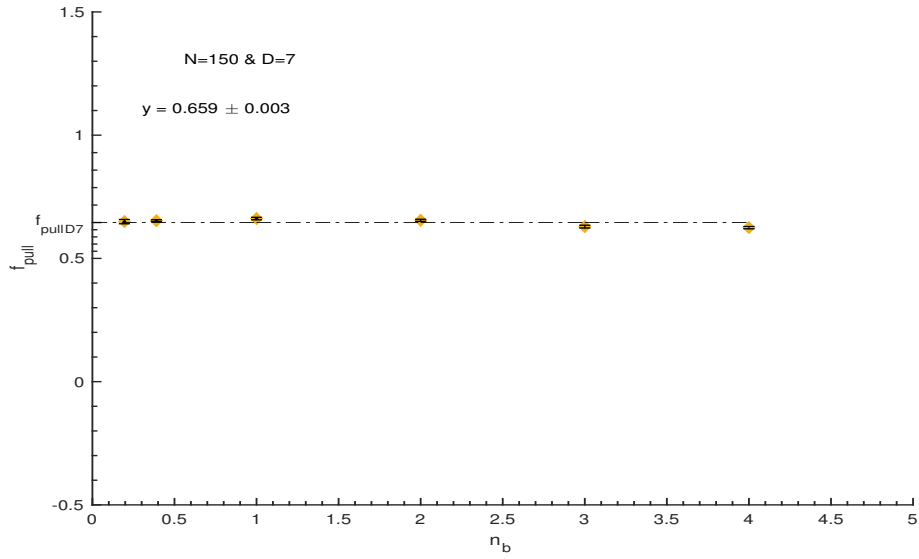


Figure 5.16: Pulling force as a function of the size of the tail.

Table 5.6: The length of the polymer inside the tube in terms of the total number of blobs

Number of blobs outside	4	3	2	1	0.66	0.33
Number of blobs inside	$6 \sim 0.6 n_b$	$7 \sim 0.7 n_b$	$8 \sim 0.8 n_b$	$9 \sim 0.9 n_b$	$9.34 \sim 0.934 n_b$	$9.67 \sim 0.967 n_b$

the seed we start with at the beginning of the simulation, and due to the pulling force from the interaction between the tail and the boundary and the fact that our polymer starts with a relaxed state, we end up with more than the initial number of monomers outside throughout the simulation. Thus we are still above the critical number of blobs outside.

Chapter 6

Polymer Near a Plane

In our simulations we obtained data revealing the relationship between the densities outside the cylindrical pore (in the case of a semi-confined polymer) to the radial distance r measured from the center of the cylinder. In this section, we look forward to retrieve an analytical expression of the mentioned relationship and compare to our results. However, it should be specified that the calculations are done for an ideal chain near an infinite flat surface. Any notes concerning the corrections resulting from the fact that our chain is non-ideal and from the finite boundary case will be discussed later.

6.1 "Grafted" Chain to a Non-Adsorbing Wall

Let us consider a chain with length N and one end fixed at height $h(x, \mathbf{R})$, (refer to fig.(6.1)) [16] The thermodynamic properties are represented by the propagator G_N that satisfies the following Edwards equation [17],

$$\frac{\partial G_N}{\partial N} = \frac{a^2}{6} \Delta G_N \quad (6.1)$$

with the following boundary conditions,

$$\begin{cases} G_N(\mathbf{r}, \mathbf{r}') \equiv 0 \text{ (at the surface)} \\ \lim_{N \rightarrow 0} G_N(\mathbf{r}, \mathbf{r}') = \delta(\mathbf{r} - \mathbf{r}') \end{cases} \quad (6.2)$$

For the case of an ideal polymer with one end fixed at h the weight is found to be the following using the method of images [18]

$$G(\mathbf{h}, \mathbf{r}, N) = \left(\frac{1}{4\pi DN} \right)^{d/2} \exp\left(\frac{-R^2}{4DN} \right) \times \left[\exp\left(-\frac{(x-h)^2}{4DN} \right) - \exp\left(-\frac{(x+h)^2}{4DN} \right) \right] \quad (6.3)$$

with d dimensions, and $D = \frac{a^2}{2d}$. If $d = 3$ (as in our case) then $D = \frac{a^2}{6}$. Replacing in eq.(6.3) we get our general Green's function in terms of x , R and the number of monomers outside the pore, N . Let us assume that the size of the monomer a is 1, and the height $h = (1, 0)$. We can think of the weights as the probability of finding a monomer at a certain distance from the plane and having the following general expression,

$$G|_{h=(1,0)} = \left(\frac{3}{2\pi N} \right)^{3/2} \exp\left(\frac{-3R^2}{2n} \right) \times \left[\exp\left(-\frac{3(x-1)^2}{2n} \right) - \exp\left(-\frac{3(x+1)^2}{2n} \right) \right] \quad (6.4)$$

One essential property of the Green's function that we are dealing with is the composition law,

$$G_N(\mathbf{r}, \mathbf{r}') = \sum_s G_N(\mathbf{r}', s) G_N(s, \mathbf{r}) \quad (6.5)$$

where s could be defined as the point of contact between the polymer chain and the surface through some monomer i . Following this, we are able to divide our chain into

two sections (see sketch in fig.(6.1)):

Section A: which we define as the loop, with one end fixed at $h = (1, 0)$, ends at s and includes n monomers.

Section B: which we define as the tail, starts at s , ends anywhere and includes $N-n$ monomers. (N being the total number of monomers in the chain).

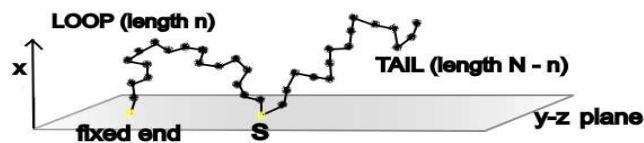


Figure 6.1: Sketch of a grafted polymer chain near a non-adsorbing surface

6.1.1 The Loop

We know that the loop is fixed at one end at $x = 1, R = 0$ and should end at an arbitrary R at s . However, we know that s is the point of contact so consequently, the loop ends at $x = 1$ too. This gives us a specific form for the Green's function corresponding to the loop by replacing x by 1 in eq.(6.4). What we need to be doing next is integrating the Green's function to get the partition function. However, we must note that to get the "number of contacts" or the weight of a contact happening

($Weight_{Loop}$) one must first multiply the Green's function by the area of the "ring" with infinitesimal thickness at which the contact appears, then we integrate over θ .

$$Weight_{Loop} = \int_0^{2\pi} \left(\frac{3}{2\pi N} \right)^{3/2} \exp\left(\frac{-3R^2}{2n}\right) \times \left[1 - \exp\left(\frac{-6}{n}\right) \right] R dR d\theta \quad (6.6)$$

$$Weight_{Loop} = \frac{3\pi\sqrt{6}}{2} \left(\frac{1}{\pi n} \right)^{3/2} \left[1 - \exp\left(\frac{-6}{n}\right) \right] \exp\left(\frac{-3R^2}{2n}\right) R dR \quad (6.7)$$

If we use Taylor expansion on the first exponential term in eq.(6.7) for large n we get the final form for the loop's partition function,

$$Weight_{Loop} = \frac{9R\sqrt{6}}{2} \frac{e^{\left(\frac{-3R^2}{2n}\right)}}{n^{5/2}} dR \quad (6.8)$$

We do not integrate over R and n yet because we still need the whole picture which includes the second partition; the tail.

6.1.2 The Tail

We are aware that the tail starts at s (contact with the surface) and ends anywhere in x and R . To produce its partition function we use the Green's function in eq. (6.4); however, $x \neq 1$ because we are not certain that the end monomer of the tail ends at the surface. On this account, we integrate over $x : 0 \rightarrow \infty$, $\theta : 0 \rightarrow 2\pi$ and $R : 0 \rightarrow \infty$.

$$Weight_{Tail} = \int_0^{2\pi} \int_0^{\infty} \int_0^{\infty} G|_{h=(1,0)} R dR dx d\theta \quad (6.9)$$

Note that the number of monomers in the tail is $N-n$,

$$Weight_{Tail} = erf\left(\frac{1}{2}\sqrt{\frac{6}{N-n}}\right) \quad (6.10)$$

To simplify eq. (6.10) we use Puiseux series to expand it for large values of $N-n$,

$$Weight_{tail} = \sqrt{\frac{6}{\pi}}\sqrt{\frac{1}{N-n}} \quad (6.11)$$

6.1.3 Weight of Contact

Now that we have the weights for the two divisions (loop and tail), and following from the composition law in eq.(6.5), we need only multiply their corresponding partition functions that are thus far dependent on R and n . Additionally, we integrate over n such that we end up with the distribution of contacts (let us call it $C(R)$) that has a fixed total number of monomers N , with respect to the radial position R only.

$$C(R) = \int_0^N \frac{54R}{\pi} \frac{e\left(\frac{-3R^2}{2n}\right)}{n^{5/2}(N-n)^{1/2}} dn \quad (6.12)$$

As the reader can see, for small values of n we have a small loop and a large tail and thus we have a contact close to the origin, and the opposite also holds for large values of n . A simple change of variable where $t = n/N$ would render the integral as follows (where $t \in 0 \rightarrow 1$ for $n \in 0 \rightarrow N$),

$$C(R) = \int_0^1 \frac{54R}{\pi} \frac{e\left(\frac{-3R^2}{2tN}\right)}{t^{5/2}N^2(1-t)^{1/2}} dt \quad (6.13)$$

Integrating would give us,

$$C(R) = 6\sqrt{\frac{6}{\pi}} \frac{(1 + 3R^2/N)e^{-3R^2/2N}}{R^2\sqrt{N}} \quad (6.14)$$

Studying eq. (6.14) along the radial direction would allow us to compare to the results of densities of forces and contacts in our MD simulations; section (6.2).

Now, if we consider eq. (6.14) to describe the magnitude of the force along the radial direction, then integrating over R should present us with an expression (let us call it \hat{f}) that portrays the average of that force which we call the pulling force. We integrate from $D \rightarrow \infty$ since there is no possibility of contact at the opening of the cylinder where $R < D$. The expression is as follows,

$$\hat{f} = \frac{6\sqrt{6}e^{-3D^2/2N}}{D\sqrt{\pi N}} \quad (6.15)$$

To observe the importance of eq.6.15 let us recall the expression of f_{pull} ,

$$f_{pull} = \frac{Bk_B T}{D} \quad (6.16)$$

It is remarkable that we were able to reproduce this dependence on $1/D$ without deriving it from the free energies and without the help of scaling arguments.

6.2 Comparison with MD results

To obtain the "concentration" of forces and contacts in our MD simulations we set the total number of monomers, the diameter and the number of blobs we desire to be outside. From the latter we get N_{out} which is the number of monomers outside the tube and in contact with the outer flat plane. We use N_{out} in plotting later on the theoretical concentrations in eq.(6.14). During the simulation we record any "contact" or interaction that happens with the outer boundary along with its position and magnitude. We

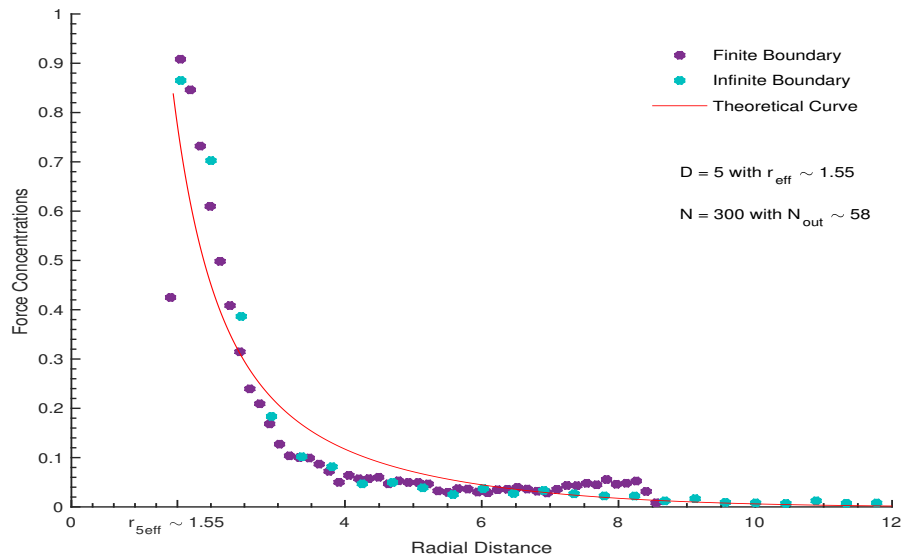
then take the range of the radial distance on which interactions occur and segregate it into bins of equal thickness. Afterwards, we sort the frequency and magnitude of the interaction accordingly. The final step is to normalize all the data and the theoretical curve such that the integral over the curves produce the magnitude of the total force associated with diameter being used.

All the data shown is for $N = 300$. Figures (6.2a) and (6.2b) show the concentration profile for the forces and contacts respectively, for $D = 5$.

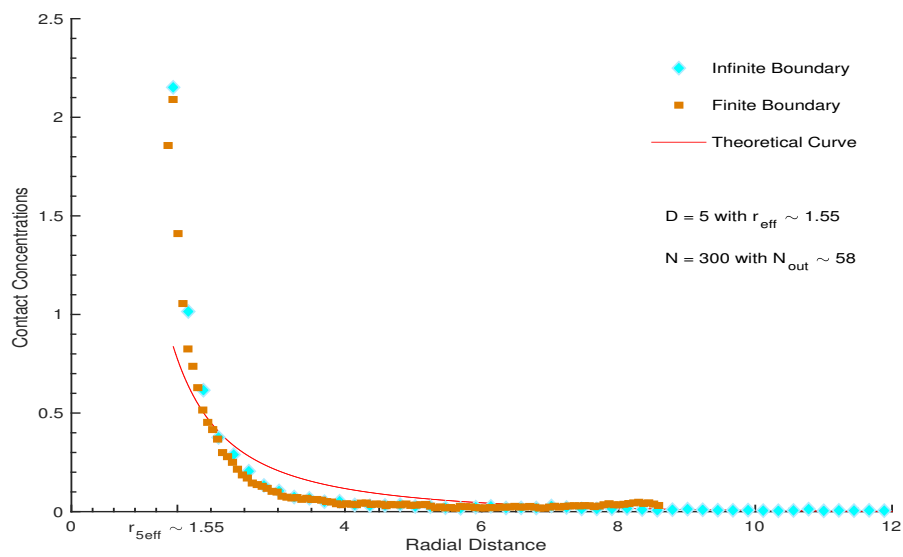
The results for $D = 7$ is shown in fig.(6.3), and those for $D = 12$ in fig.(6.4). The first thing we notice from the figures below is that they all validate the value of D_{eff} we chose for our system in our previous studies. If we take for example a cylinder of diameter 12, we expect the effective diameter to be $D_{eff} = D - 1.9 = 10.1$ thus the radius is ~ 5.05 , which is the case in fig.6.4. Another prominent point is the difference between the infinite and finite outer boundaries. The radial distance at which the finite curve ends is close to the outer edge of the outer cylinder which is at a distance equal to $D + thickness + 2^{1/6}$, with $thickness = 5$ in all three figures. The "bumps" we see at the end of the curve can be explained as follows: the polymer chain is getting closer to the wall and experiencing repulsion, then it starts exploring greater radial distances until it reaches the curve which is a partition between repulsive walls and free space to explore. The polymer tends to explore the free space in the region close to the cutoff distance of our potential and comes close enough such that the amplitude of contacts and force is no longer zero.

This brings us to the subject of amplitudes. If we try to compare the curves of forces to those of contacts, we can see that at the same radial distance r , we have greater amplitudes for the contacts than for the forces. This indicates that even though we have a large number of contacts, most of their contribution to the force is minimal.

Moreover, the fact that the two curves (infinite and finite) overlap answers the question

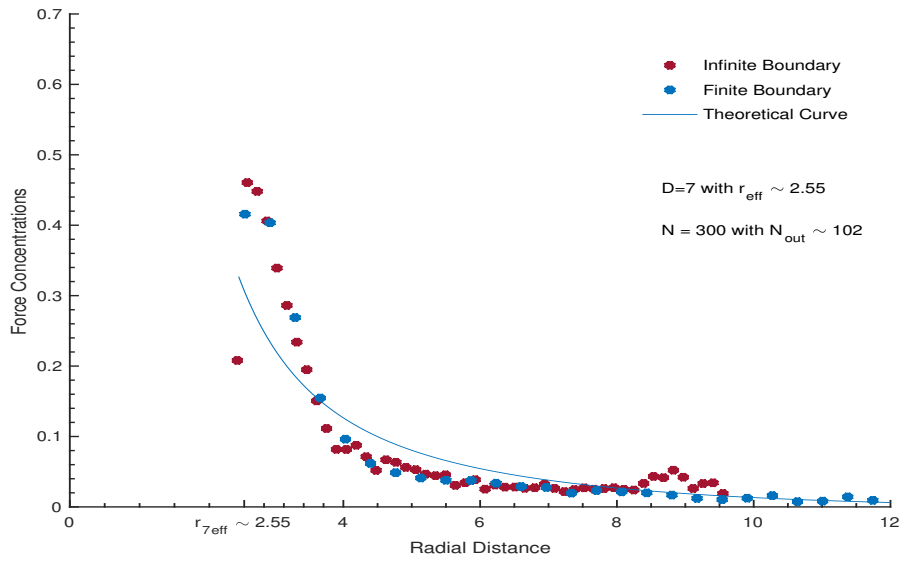


(a)

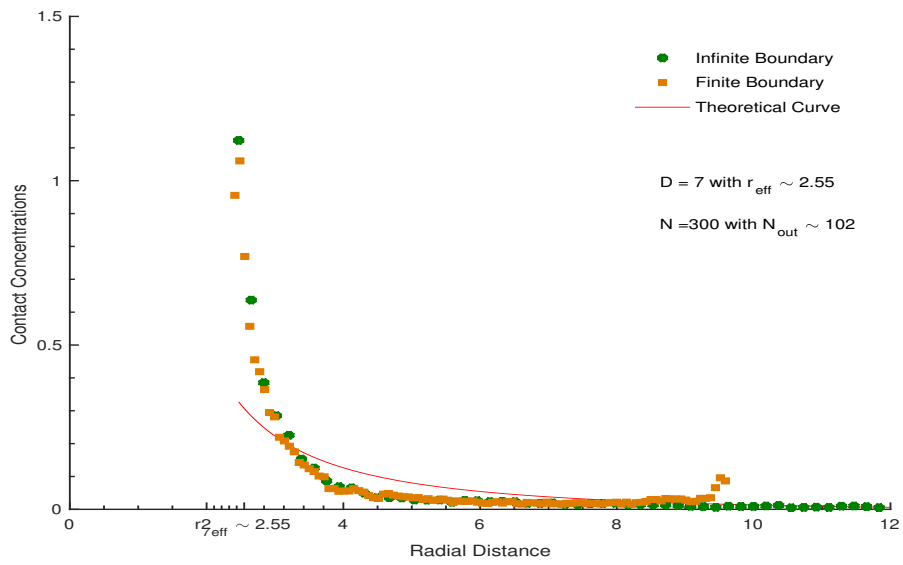


(b)

Figure 6.2: The Concentration of forces (a) and contacts (b) of interaction for $N = 300$ and $D = 5$ for infinite and finite outer boundaries

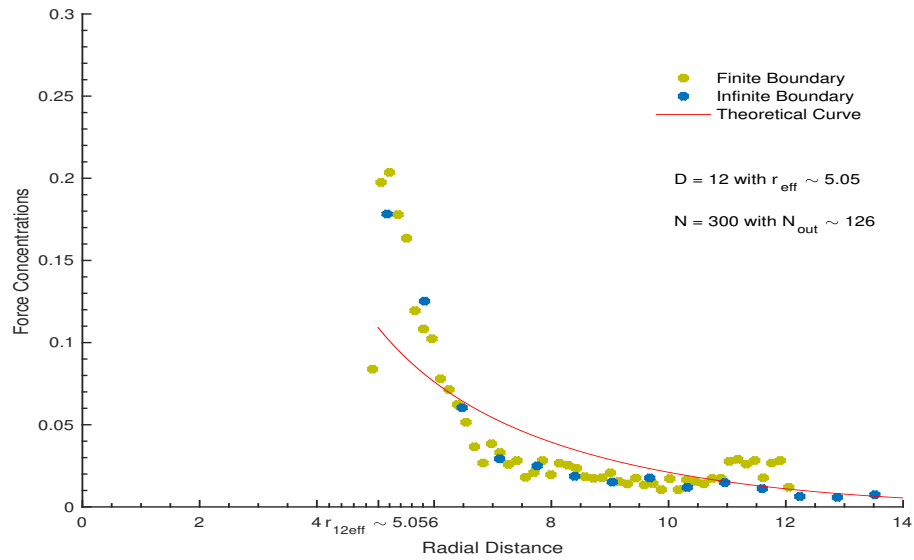


(a)

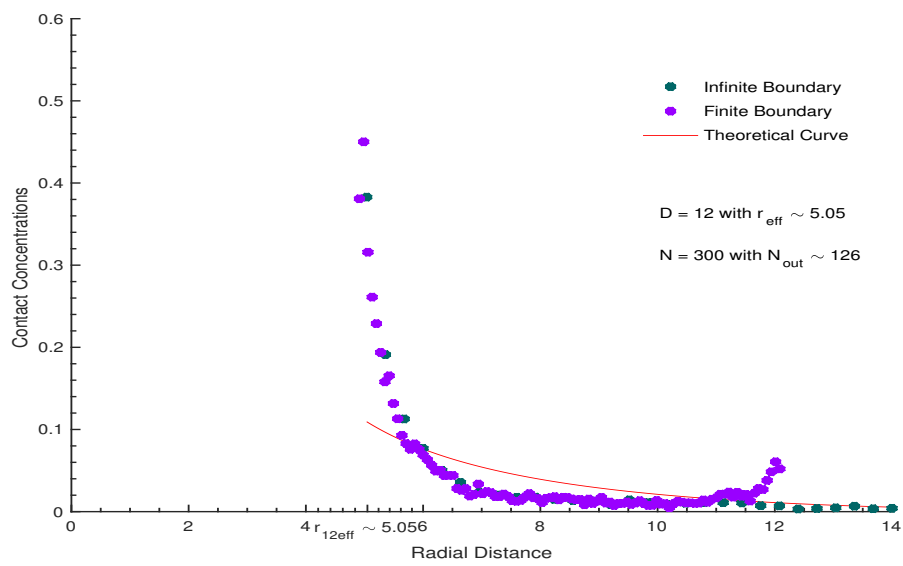


(b)

Figure 6.3: The Concentration of forces (a) and contacts (b) of interaction for $N = 300$ and $D = 7$ for infinite and finite outer boundaries



(a)



(b)

Figure 6.4: The Concentration of forces (a) and contacts (b) of interaction for $N = 300$ and $D = 12$ for infinite and finite outer boundaries

of these limiting cases that we first asked in this thesis research; do the two cases result in the same pulling force and do they have equal free energies?

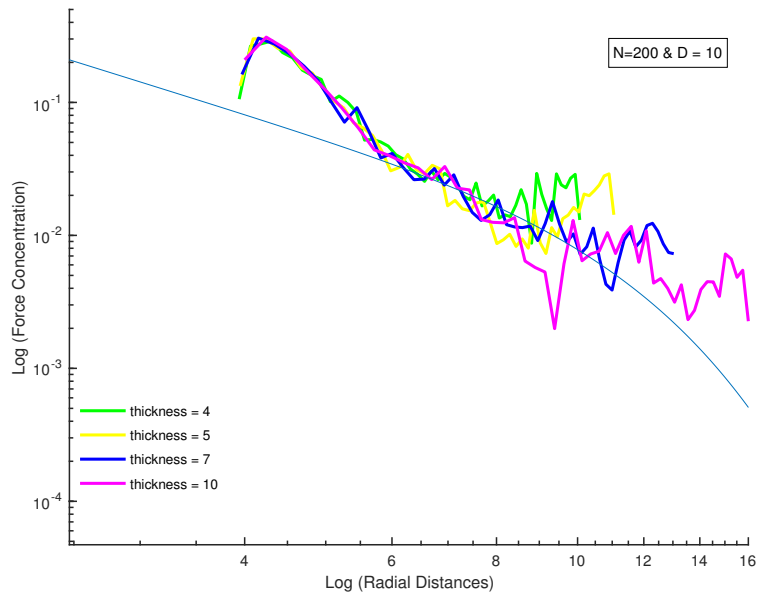


Figure 6.5: $\text{Log}_{10} - \text{Log}_{10}$ plot of the force concentration against the radial distance for $N = 200 / D = 10$ with finite boundaries of different thicknesses

Fig.(6.5) shows the force concentration for several values of the thickness h for the finite boundary case. All these curves belong to $D = 10$ thus they produce the same pulling force. Eventhough the curve with higher values of the thickness h extend to larger radial distances, we can see that for each case there exists a sudden decrease in the force making up for it.

The last remark concerning this topic deals with the discrepancies we see in figures (6.2-6.4) between the theoretical curve and the simulation. We must note that while calculating the theoretical results, we assumed that we are dealing with an ideal chain, and all corrections of excluded volume were ignored. In addition to that, we assumed that the chain is grafted at the center $(0,0)$ of the opening of the tube and is not free

to move across the diameter. The effects of the latter are easily seen as we go to larger diameters where in real life the polymer has more space to explore and is free to position itself at places other than the center. To support the latter claim we plot the densities of the end monomers at the open end of the tube along the radial distance and we see in fig.(6.6) that the end monomers as said before are free to move along the radial direction at distances below r_{eff} .

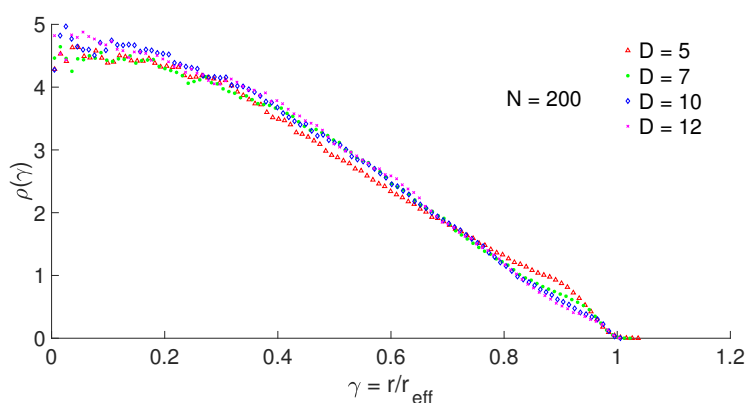


Figure 6.6: A plot of the densities of monomers near the open end of the tube along the radial direction for $D = 5, 7, 10, 12$

Chapter 7

A Brief Analogy to Biological Systems

A thorough understanding of entropic forces is important in various areas of both science and technology. One can subsequently relate them to transfer of polymers in biological systems such as the separation of DNA molecules in the course of meiosis or the ejection of DNA from a bacteriophage. In this chapter, we will use the latter to provide a biophysical analogy to the polymer physics we have studied this far, and to demonstrate its application to other fields as well.

If we take a look at a bacteriophage's structure fig.(7.1, we can see that the tail of the phage closely resembles the cylindrical nanopore in our model. It has been shown that the in vitro DNA ejection of a bacteriophage T5 can be provoked by the interaction with its receptor. A T5 phage has a close resemblance to our model, because it contains linear dsDNA along with a long non-contractile tail [19]. Once the trigger of an in vitro T5 DNA ejection is administered, the base plate of the phage binds to the E. coli receptor [20]. This process prompts a signal to the connector found between the head and tail such that it opens and allows the release of the DNA. We are interested in the process where the DNA is existing the end of the tail through the base plate and

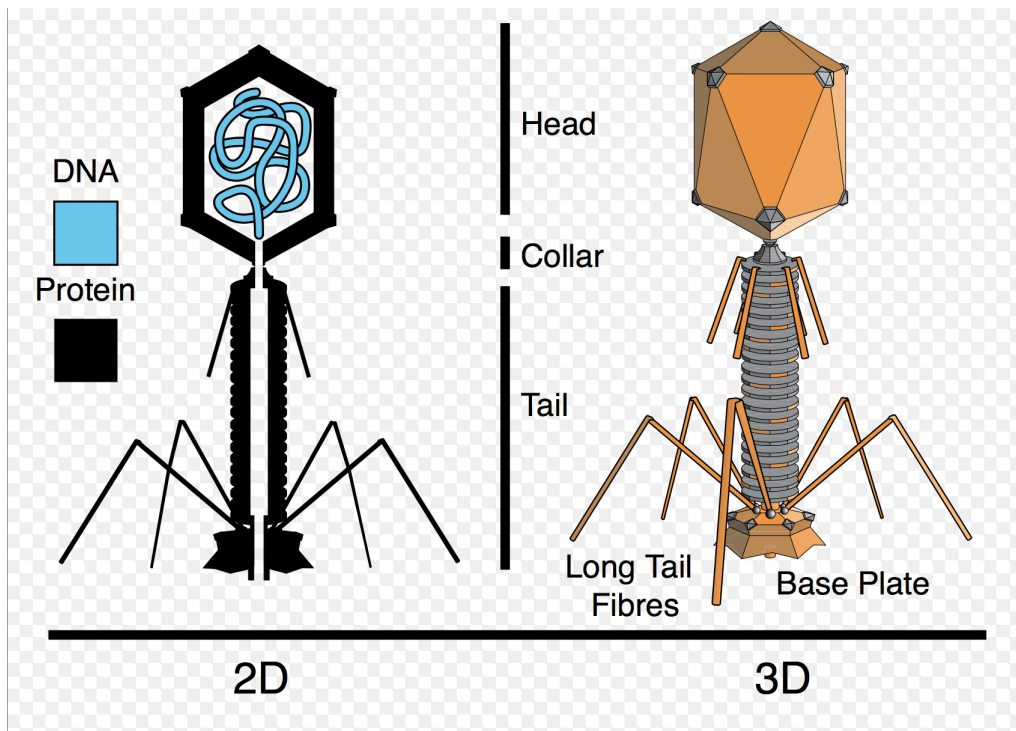


Figure 7.1: A 2D and 3D image of the structure of a bacteriophage

getting ready for the infection process. Recent in vitro studies show that the dsDNA being ejected experiences a driving force f_{eject} (f_{pull} in our model). However, this force can be repressed by external osmotic pressure creating a resistive force f_{resist} (f_{spring} in our model) prohibiting the entry of the DNA into the solution [21]. In vivo experiments are hard to administer; however, comparing in vivo and in vitro ejections to our limiting cases might help us in setting a model based prediction.

In vitro ejections usually take place from confinement (capsid) to salty solutions, where the latter can be considered as free space. This resembles the limiting case with infinitesimal outer boundaries, where the thickness of the wall h can be related to the thickness of the protein layer surrounding the base plate and tail. Whereas in in-vivo ejections the base plate attaches to the host cell and the ejection takes place in the host cell's cytoplasm, and the host cell walls act as "infinite" boundaries to the DNA

strand.

The results of our model's limiting cases, along with their analogy to the biological process stated above can help us predict that if a resistive force preventing ejection can occur in in-vitro DNA ejection for an environment of certain characteristics, then in-vivo DNA ejection would experience the same ejecting and resisting forces for the same parameters.

Chapter 8

Summary, Conclusion and Future

Work

In this thesis research we presented a study of fully and semi-confined polymer chains placed in a nanopore of diameter D , length L (in semi-confined case), and with impenetrable repulsive walls. We utilized MD simulations to retrieve global chain characteristics in full confinement, along with extracting measurements and dependencies of radial, pulling and entropic forces and free energies in semi-confined chains for our two limiting cases (finite and infinite boundary walls at the open end). Our results were briefly as follows:

1. Free Polymer Chain

- The end-to-end distance (R_{ee}) dependence on N was extracted and shown to be $R_{ee} \sim N^{0.61}$, where N is the number of monomers.
- The relaxation times of a free polymer demonstrated an agreement with theoretical scaling laws concerning the dependence on N , $\tau_{rel} = N^{2.27}$.

2. Fully Confined Chain

- We found a nonuniversal correction to the pore's diameter D that shifts it to $D - \delta$ (effective diameter D_{eff}) with $\delta = 1.9$.
- The dependence of the end-to-end distance (R_{ee}) was deduced to scale as $R_{ee} \sim CN^{1.1}D^{-0.78}$ compared to the theoretical scaling law with $R_{ee} \sim CND^{-0.67}$ where C is a model dependent constant. Our simulations are in agreement with the theory taking into account the errors on our data. Extracting the constant C from our model, we got $C = 1.11 \pm 0.08$ and 1.20 ± 0.04 from two different methods.
- Studing the radial force acting on the confined polymer we deduced that we were not able to reach the correct asymptotic limits for the scaling law ,instead, we arrived at $f_{radial} \sim AN^{0.78}D^{-2.3}$. f_{radial} is not yet linear in N and this leads to a dependence of the ratio of f_{radial}/R_{ee} on the number of monomers N , whereas this dependence does not exist in theory. The model dependent amplitude A was calculated and found to be $A = 2.8 \pm 0.09$ and $A = 2.14 \pm 0.04$ from two different methods.
- We know that the ratio A/C should produce a universal constant $B = 5.79$, yet the values we have do not manufacture that. Thus, we conclude that we need to go to higher values of N and stronger confinement to retrieve the theoretical value of B and the dependence of f_{radial} on the number of monomers and the diameter.
- The relaxation times of a confined chain in our model were shown to be $\tau_{rel} \sim N^{2.03}D^{1.14}$ which agrees with the theory for the dependence on N yet we observe a much stronger dependence of the diameter than expected. Taking into consideration that other MC (Monte Carlo) simulations were able to reach higher degrees of polymerization and stronger confinement

but still were not able to reach the theoretical asymptotic limits, we cannot be certain that going for larger N would eventually lead to the theoretical scaling law. However, doing so is one of the viable solutions.

3. Semi-Confined Chain

- Theoretical predictions suggesting that the mean pulling force for our two limiting cases is the same, are proven to be correct. Our results show homogeneity between the resultant pulling forces from the two cases for different values of N and more importantly of the diameter.
- The pulling force's dependence on the diameter and the temperature has been obtained rather precisely and shown to be $f_{pull} \sim \tilde{B}T^{0.92}/D^{1.06}$.
- Using several methods we deduce that the coefficient \tilde{B} in the expression of the pulling force is not the universal model independent constant B , and it turns out that $\tilde{B} \sim 3.2$.
- We extract B from the fully confined pull method and our results show it to be $B = 5.34 \pm 0.07$.
- We deduced that the free energy per unit length for full confinement is larger than that for semi-confinement.
- Our simulations show a relation between f_{radial} and f_{pull} to be $f_{radial} = 2Lf_{pull}/D$

4. Polymer Near a Plane

- From the Green's function near a plane, we deduce the change of the densities of forces and contacts with radial distance. From the latter we extract an expression that retrieves the dependence of the force on the diameter D .

- When comparing the theoretical expression of the densities to the simulation results we find an overlap between the curves of the finite and infinite boundaries resulting with an equal pulling force. The simulations further support our choice of the effective diameter.

For future work, we could begin with reaching the asymptotic limits for confined polymers with taking higher values of N (as much as affordable MD simulations would allow). We also plan on enhancing the expression of the concentrations near the repulsive wall by removing the assumption that we have a grafted monomer at the center of the open end, instead we leave it to move freely in a certain radial distance below the diameter. Finally, I would hope that one day I would be able to build the environment that replicates real biological systems and be able to simulate and study their physical aspects.

Bibliography

- [1] M. Doi, *Introduction to Polymer Physics*. Clarendon Press, Oxford, 1996.
- [2] S. Enders, K. Langenbach, P. Schrader, and T. Zeiner, “Phase diagrams for systems containing hyperbranched polymers,” *Polymers*, vol. 4, pp. 72–115, 2012.
- [3] M. Kotelyanskii and D. Theodorou, *Simulation Methods for Polymers*. CRC Press, 2004.
- [4] P. Flory, *Principles of Polymer Chemistry*. New York: Cornell University Press, 1971.
- [5] M. Daoud and P. D. Gennes, “Statistics of macromolecular solutions trapped in small pores,” *Journal de Physique*, vol. 38, pp. 85–93, 1977.
- [6] P. D. Gennes, *Scaling Concepts in Polymer Physics*. Cornell University Press, 1979.
- [7] A. Milchev, L. Klushin, A. Skvortsov, and K. Binder, “Ejection of a polymer from a nanopore: Theory and computer experiment,” *Macromolecules*, vol. 43, pp. 6877–6885, 2010.
- [8] L. Klushin, A. Skvortsov, H. Hsu, and K. Binder, “Dragging a polymer chain into a nanotube and subsequent release,” *Macromolecules*, vol. 41, pp. 5890–5898, 2008.

- [9] D. Dimitrov, A. Milchev, K. Binder, L. I. Klushin, and A. M. Skvortsov, “Universal properties of a single chain in a slit: Scaling versus molecular dynamics simulations,” *The Journal of Chemical Physics*, vol. 128, 2008.
- [10] F. Brochard and P. G. de Gennes, “Dynamics of confined polymer chains,” *The Journal of Chemical Physics*, vol. 67, 1977.
- [11] A. Arnold, B. Bozorgui, D. Frenkel, B. Ha, and S. Jun, “Unexpected relaxation dynamics of a self-avoiding polymer in cylindrical confinement,” *The Journal of Chemical Physics*, vol. 127, 2007.
- [12] M. Rubenstein and R. Colby, *Polymer Physics*. Oxford University Press, 2003.
- [13] T. Burkhardt and I. Guim, “Free energy of a long, flexible, self-avoiding polymer chain in a tube,” *Phys. Rev. E*, vol. 59, no. 5, pp. 5833–5838, 1999.
- [14] D. Rapaport, *The Art of Molecular Dynamics Simulation*. Cambridge University Press, 2004.
- [15] D. Frenkel and B. Smit, *Understanding Molecular Simulation: From Algorithms to Applications*. Academic Press, 2001.
- [16] T. Bickel, C. Jeppensen, and C. Marques, “Local entropic effects of polymers grafted to soft interfaces,” *Eur. Phys. J. E*, vol. 4, pp. 33–44, 2001.
- [17] M. Doi and S. Edwards, *The Theory of Polymer Dynamics*. Clarendon Press, Oxford, 1986.
- [18] S. Chandrasekhar, “Stochastic problems in physics and astronomy,” *Reviews of modern physics*, vol. 15, no. 1, p. 1, 1943.

- [19] S. M. Grath and D. van Sinderen, *Bacteriophage: Genetics and Molecular Biology*. Caister Academic Press, 2007.
- [20] M. de Frutos, L. Letellier, and E. Raspaud, “Dna ejection from a bacteriophage t5: Analysis of the kinetics and energetics,” *Biophysical Journal*, vol. 88, pp. 1364–1370, 2005.
- [21] A. Evilevitch, L. Lavelle, C. M. Knobler, E. Raspaud, and W. M. Gelbart, “Osmotic pressure inhibition of dna ejection from phage,” *Proc. Natl. Acad. Sci. USA*, vol. 100, pp. 9292–9295, 2003.